stresses

MDPI

Article

Exploring Epigenetic Modifiers in Cowpea: Genomic and Transcriptomic Insights into Histone Methyltransferases and Histone Demethylases

Jéssica Barbara Vieira Viana [1], José Ribamar Costa Ferreira-Neto [1,*], Eliseu Binneck [2], Roberta Lane de Oliveira Silva [1], Antônio Félix da Costa [3] and Ana Maria Benko-Iseppon [1,*]

[1] Laboratório de Genética e Biotecnologia Vegetal, Center of Biosciences, Genetics Department, Federal University of Pernambuco, Av. Prof. Moraes Rego, 1235, Recife 50670-901, PE, Brazil; jessbarbara.jb@gmail.com (J.B.V.V.); lane.roberta@gmail.com (R.L.d.O.S.)
[2] Embrapa Soja—Brazilian Agricultural Research Corporation (Embrapa), Rodovia Carlos João Strass—Distrito de Warta, Londrina 86085-981, PR, Brazil; eliseu.binneck@embrapa.br
[3] Pernambuco Agronomic Institute, Av. Gen. San Martin, 1371—Bongi, Recife 50761-000, PE, Brazil; felix.antonio@ipa.br
* Correspondence: joseribamar.ferreiraneto@ufpe.br (J.R.C.F.-N.); ana.iseppon@ufpe.br (A.M.B.-I.)

Abstract: Histone methyltransferases (SDGs) and demethylases (JMJs) are well-established regulators of transcriptional responses in plants under adverse conditions. This study characterized SDG and JMJ enzymes in the cowpea (*Vigna unguiculata*) genome and analyzed their expression patterns under various stress conditions, including root dehydration and mechanical injury followed by CABMV or CPSMV inoculation. A total of 47 VuSDG genes were identified in the cowpea genome and classified into seven distinct classes: I, II, III, IV, V, VI, and VII. Additionally, 26 VuJMJ-coding genes were identified and categorized into their respective groups: Jmj-only, JMJD6, KDM3, KDM5, and KDM4. Analysis of gene expansion mechanisms for the studied loci revealed a predominance of dispersed duplication and WGD/segmental duplication events, with Ka/Ks ratios indicating that all WGD/segmental duplications are under purifying selection. Furthermore, a high degree of conservation was observed for these loci across species, with legumes displaying the highest conservation rates. Cis-Regulatory Element analysis of VuSDG and VuJMJ gene promoters revealed associations with Dof-type and bZIP transcription factors, both of which are known to play roles in plant stress responses and developmental processes. Differential expression patterns were observed for VuSDG and VuJMJ genes under the studied stress conditions, with the highest number of upregulated transcripts detected during the root dehydration assay. Our expression data suggest that as the referred stress persists, the tolerant cowpea accession decreases methylation activity on target histones and shifts towards enhanced demethylation. This dynamic balance between histone methylation and demethylation may regulate the expression of genes linked to dehydration tolerance. During the mechanical injury and viral inoculation assays, VuSDG and VuJMJ transcripts were upregulated exclusively within 60 min after the initial mechanical injury combined with CABMV or CPSMV inoculation, indicating an early role for these enzymes in the plant's defense response to pathogen exposure. The current study presents a detailed analysis of histone modifiers in cowpea and indicates their role as important epigenetic regulators modulating stress tolerance.

Keywords: legume plant; drought; pathogen; virus; epigenetics

check for updates

Academic Editor: Magda Pál

Received: 4 December 2024
Revised: 6 February 2025
Accepted: 8 February 2025
Published: 13 February 2025

Citation: Viana, J.B.V.; Ferreira-Neto, J.R.C.; Binneck, E.; Oliveira Silva, R.L.d.; Costa, A.F.d.; Benko-Iseppon, A.M. Exploring Epigenetic Modifiers in Cowpea: Genomic and Transcriptomic Insights into Histone Methyltransferases and Histone Demethylases. *Stresses* **2025**, *5*, 13. https://doi.org/10.3390/stresses5010013

Copyright: © 2025 by the authors. Licensee MDPI, Basel, Switzerland. This article is an open access article distributed under the terms and conditions of the Creative Commons Attribution (CC BY) license (https://creativecommons.org/licenses/by/4.0/).

1. Introduction

In eukaryotes, DNA associates with proteins known as histones. Initially, the proposed role of this protein group was limited to compacting genetic material by forming nucleosome structures [1]. However, subsequent research revealed that histones are not inert molecules but serve as substrates for post-translational modifications. These chemical (epigenetic) modifications occur on specific amino acid residues in the N-terminal tails of histones, affecting their interaction with DNA. Consequently, this modulates the accessibility of transcriptional machinery to chromatin, impacting transcription factor binding interactions and, subsequently, gene expression.

A wide array of post-translational histone modifications has been cataloged (reviewed by Ferreira-Neto et al. [2]). Among these, histone methylation and demethylation are particularly significant in plants, serving as relevant epigenetic regulators of gene expression during development and in stress response.

In plants, histone methylation involves the addition of up to three methyl groups to specific lysine (K) residues, a process catalyzed by histone methyltransferases (HKMTases). These residues include K4, K9, K27, K36, and K79 on histone H3 and K20 on histone H4 [3,4]. HKMTases, also known as SET DOMAIN GROUP (SDG) proteins, contain an evolutionarily conserved SET domain that serves as their catalytic module [5]. These enzymes can either up or downregulate gene expression, depending on the methylation state and the specific lysine residue modified [6]. For example, the addition of a single methyl group (me) to residues K4 and K36 of histone H3 (resulting in H3K4me and H3K36me, respectively) is associated with gene upregulation, while methylation of H3K9, H3K27, and H4K20 is linked to gene downregulation [4,7].

In plants, SET DOMAIN GROUP (SDG) proteins are categorized into seven distinct classes based on histone methyltransferases initially identified in Drosophila. These classes include the following: (a) Class I—E(z) homologs, responsible for catalyzing the methylation of H3K27; (b) Class II—Ash1 homologs, which catalyze the methylation of H3K36; (c) Class III—Trx homologs and related proteins, involved in the methylation of H3K4; (d) Class IV—proteins containing both SET and PHD (plant homeodomain) domains; (e) Class V—Su(var)-related and homologous proteins, which catalyze the methylation of H3K9; (f) Class VI—proteins characterized by an interrupted SET domain; and (g) Class VII—Rubisco methyltransferase (RBCMT) [5].Histone methylation is a dynamic process, as methyl groups on lysine residues can be removed via demethylation [8]. This process is facilitated by histone demethylase enzymes containing the JmjC domain, also known as JMJ proteins, which employ Fe(II)- and α-ketoglutarate (α-KG)-dependent hydroxylation reactions [9,10]. In *Arabidopsis thaliana*, JMJ proteins are classified into five categories based on sequence similarity and specificity for methylation marks: (a) KDM4, which includes the PKDM8 and PKDM9 subgroups, targets the demethylation of H3K9me2/3 and H3K36me2/3 marks, respectively; (b) KDM5, responsible for the demethylation of H3K4me1/2/3; (c) JMJD6, which acts on the demethylation of H3K27me2/3; (d) KDM3, which demethylates H3K9me1 and H3K9me2; and (e) JmjC domain-only enzymes, represented by the PKDM11/12/13 subclasses, which specifically target H3K27me3 demethylation [11,12].

Studies indicate that SDG and JMJ proteins regulate various plant biological processes, including responses to environmental stresses such as drought [13], cold [14], high temperature [15], salinity [16], and pathogen attack [17]. The genomic identification and functional analysis of SDG and JMJ proteins is an emerging field, studied across species such as *A. thaliana* [5], rapeseed (*Brassica rapa*) [18], rice (*Oriza sativa*) [19], tomato (*Solanum lycopersicum*) [20], maize (*Zea mays*) [15,21], citrus [22], soybean (*Glycine max*; the only legume analyzed in this context) [23], apple (*Malus domestica*) [24], cotton (*Gossypium raimondii* and

Gossypium hirsutum) [25,26], and wheat (*Triticum aestivum*) [27]. Most studies have focused on either the SDG or JMJ family individually; to date, only Aiese et al. [20], Xu et al. [22], and Fan et al. [24] have analyzed both gene families using both genomic and transcriptomic approaches, allowing a direct comparative analysis, particularly at the gene expression level under specific conditions.

Cowpea (*Vigna unguiculata* [L.] Walp.), a legume plant widely cultivated in Africa and Brazil, is economically and nutritionally significant, providing essential protein, minerals, and carbohydrates to low-income populations [28,29]. Additionally, some cowpea accessions exhibit tolerance to drought and high temperatures, making them well-suited for semi-arid, non-irrigated regions [29]. However, studies on the structural and functional characterization of SDG and JMJ proteins in the mentioned crop are currently lacking. With the release of the cowpea reference genome [30], this species has entered the omics era. Furthermore, the Cowpea Genomics Consortium (CpG), managed by our research group, offers transcriptomic data from stress-tolerant cowpea accessions under conditions like root dehydration and multiple stress combinations [mechanical injury followed by virus inoculation with CABMV (*Cowpea aphid-borne mosaic virus*) or CPSMV (*Cowpea severe mosaic virus*)]. These stressors significantly impact commercial cowpea crops. Integrating genomic and transcriptomic data thus provides a valuable platform for SDG and JMJ analysis in cowpea, potentially unlocking crucial biological insights with biotechnological applications.

In light of these points, this study aimed to characterize the genomic and transcriptomic profiles of the SDG (VuSDG) and JMJ (VuJMJ) gene families in cowpea. Our results offer a comprehensive overview of these protein families, laying the groundwork for further experimental exploration of SDG and JMJ proteins in this strategic legume species.

2. Results

2.1. Genomics

2.1.1. Identification and Classification of VuSDGS and VuJMJs in the Cowpea Genome

Forty-seven VuSDGs-coding genes were identified in the scrutinized genome, each containing the catalytic SET domain (PF00856). Based on the identification of additional domains (AWS, WIYLD, Pre-SET, PHD, PWWP, FYRC, FYRN, Post-SET, Zf-CW, CXC, and SANT), the VuSDGs were categorized into seven distinct classes: I, II, III, IV, V, VI, and VII (Table S1). Classes V and VII were the most represented, with 11 and 10 genes, respectively (Table S1).

Comprehensive data on these 47 VuSDGs, including gene IDs, classifications, nucleotide lengths, polypeptide lengths, isoelectric points (pI), molecular weights (MW), and predicted subcellular localizations, are detailed in Table S2. Structurally, VuSDG proteins ranged from 310 to 2387 amino acids, with pIs from 4.34 to 9.28 and MWs between 34.59 and 169.07 kDa. The majority of VuSDGs were localized to the nucleus (36), with others in the cytoplasm (four), plasma membrane (three), extracellular space (two), chloroplast (one), and mitochondria (one) (Table S2). Additionally, 26 VuJMJs-coding genes were identified and classified according to their respective groups: Jmj-only (containing PKDM11–13 subgroups), KDM3, KDM4 (containing PKDM8–9 subgroups), KDM5, and JMJD6. Domain analysis revealed that all VuJMJs contained the JmjC catalytic domain (PF02373), while 11 also included a JmjN domain, present in all members of the KDM5, PKDM8, and PKDM9 groups. The zf-C5HC2 zinc finger domain was found in all PKDM8 and KDM5 members, while the Jmj-only class contained only the JmjC domain. FYRN and FYRC domains were also identified in most KDM5 members (Table S3).

The 26 VuJMJ proteins exhibited lengths from 413 to 1832 amino acids, with pIs between 4.93 and 8.9 and MWs ranging from 46.05 to 179.1 kDa. Like VuSDGs, the majority

of VuJMJs were nuclear (19), with others found in the chloroplast (one), mitochondria (one), plasma membrane (one), and cytoplasm (four) (Table S4).

Phenetic analysis of VuSDG protein sequences, alongside those from *A. thaliana* (AtSDGs) and rice (OsSDGs), grouped VuSDGs into 10 clusters corresponding to the seven histone methyltransferase classes (Figure 1A). These classes were numbered I through VII. This analysis supported the domain-based classification of VuSDGs. Class III contained two distinct groups, with one group comprising VuSDGIII.6 and an OsSDG homolog. Similarly, Class VI was divided into three groups, two of which included only OsSDGs and VuSDGs. The gene *VuSDGIII.5*, which was grouped with OsSDG and AtSDG homologs in Class IV (Figure 1A), was ultimately retained in Class III due to its specific Class III domain characteristics (Table S1).

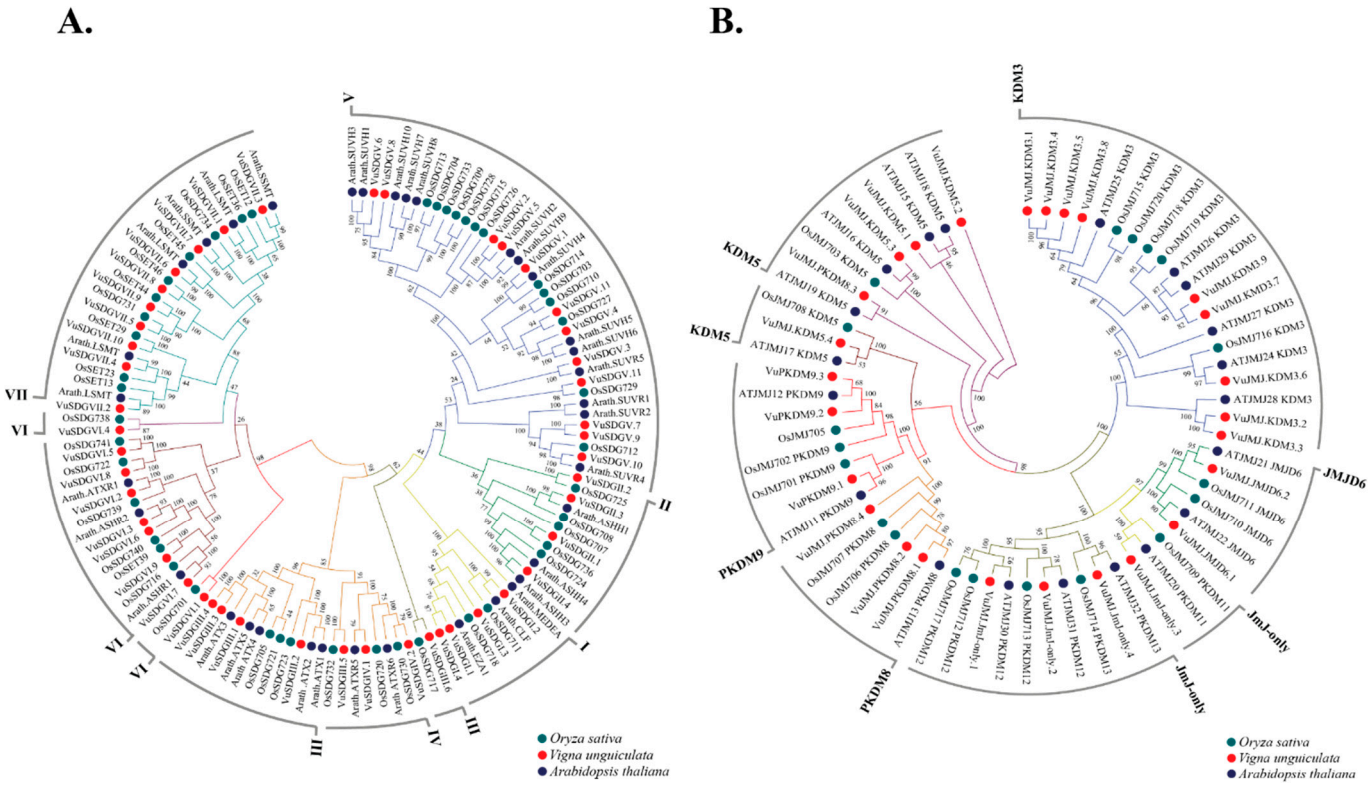


Figure 1. Neighbor-Joining trees based on the protein sequences of SDGs (**A**) and JMJs (**B**) from *Arabidopsis thaliana* (AtSDGs/AtJMJs, marked with blue circles), rice (OsSDGs/OsJMJs, marked with green circles), and cowpea (VuSDGs/VuJMJs, marked with red circles). Each protein class is represented by branches of distinct colors for easy visualization. In panel (**A**), different SDG classes are labeled with Roman numerals, while in panel (**B**), JMJ classes are identified with specific alphanumeric labels. Bootstrap values, derived from 1000 replicates, are shown at each node, indicating the statistical confidence of the phenetic relationships depicted.

The phenetic analysis of histone demethylases, which included VuJMJ protein sequences alongside those of *A. thaliana* (AtJMJs) and rice (OsJMJs), classified VuJMJ members into eight clusters spanning five histone demethylase groups (Figure 1B). These groups were designated as Jmj-only (corresponding to PKDM11, PKDM12, and PKDM13 subgroups in *A. thaliana* and rice), KDM3, JMJD6, KDM5, and KDM4 (corresponding to PKDM8 and PKDM9 subgroups). Within the phylogenetic tree, Jmj-only members formed two distinct groups: one containing *VuJMJ_Jmj-only.4* with PKDM11 homologs from AtJMJ and OsJMJ, and the other comprising VuJMJ_Jmj-only.2, *VuJMJ_Jmj-only.3*, and *VuJMJ_Jmj-only.5* alongside PKDM12 and PKDM13 members from AtJMJ and OsJMJ. The KDM4 group was split into PKDM8 and PKDM9. The KDM5 group, in turn, was further subdivided into two

groups, each comprising VuJMJ members, reinforcing the classification of VuJMJs through domain-specific identification (Table S3). Although *VuJMJ_PKDM8.3* clustered with OsSDG and AtSDG homologs within the KDM5 class (Figure 1B), domain analysis had previously assigned it to PKDM8 (Table S3). Consequently, *VuJMJ_PKDM8.3* was classified within the PKDM8 group (Table S3).

Since the PKDM8 and PKDM9 subgroups within the KDM4 group target distinct histone marks (H3K9me and H3K36me, respectively), subsequent analyses of the mentioned group will focus on these specific subgroups. Conversely, the Jmj-only group will not be further analyzed at the subgroup level, as all its members are exclusively associated with the demethylation of the same mark (H3K27me).

Mapping of the 47 VuSDGs across cowpea's 11 reference chromosomes revealed a heterogeneous distribution (Table S5; Figure 2). Certain loci, such as *VuSDGV.5*, *VuSDGVII.2*, *VuSDGII.4*, *VuSDGVII.3*, and *VuSDGVII.6*, were positioned near chromosome termini on chromosomes 2, 3, 4, 6, and 7, respectively. Additionally, two loci were mapped to pericentromeric regions on chromosomes 4 and 7 (*VuSDGVII.7* and *VuSDGV.7*, respectively). The 26 VuJMJs were distributed across eight of the eleven chromosomes, with none located on chromosomes 4, 5, or 8 (Table S6; Figure 2). VuJMJs exhibited a similarly uneven chromosomal distribution, with four loci (*VuJMJ_KDM3.8*, *VuJMJ_KDM3.7*, *VuJMJ_KDM3.4*, and *VuJMJ_KDM3.1*) situated at the subterminal position on chromosomes 3 and 7. Additionally, the *VuJMJ_PKDM9.4* locus was found in the pericentromeric region of chromosome 9.

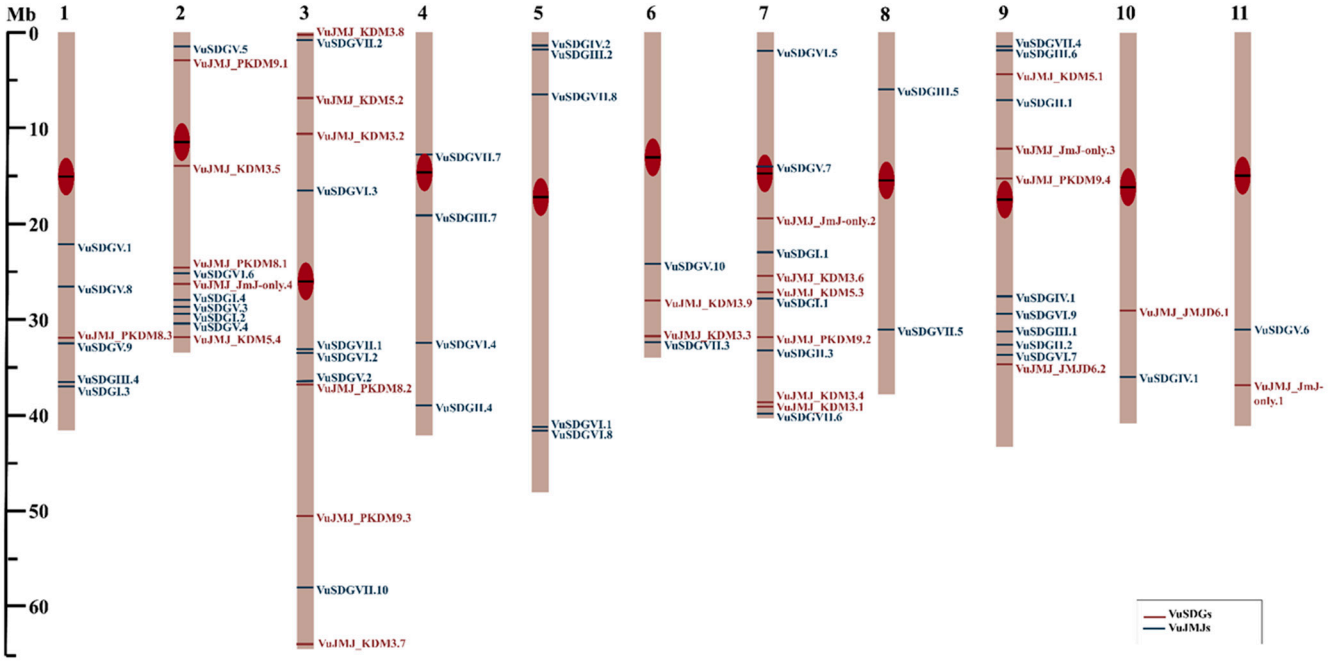


Figure 2. Chromosomal distribution of VuSDG and VuJMJ loci in the cowpea genome. Red and blue marks and labels indicate the positions of VuSDG and VuJMJ genes, respectively, along the 11 studied chromosomes. Dark red ellipses represent centromeres. Chromosome lengths are scaled to the left sidebar, denoted in megabases (Mb).

2.1.2. VuSDGs and VuJMJs Gene Structure

To characterize the structural features of the VuSDG and VuJMJ genes, we analyzed 12 parameters (Tables S7 and S8). The main gene structures, including introns, coding sequences (CDS), and untranslated regions (UTRs) for a representative sample of VuSDGs and VuJMJs, are schematically represented in Figure 3. This section highlights exon, intron, and domain counts, as these features are particularly informative.



Figure 3. Gene structures of a representative sample of VuSDG (**A**) and VuJMJ (**B**) genes. Different classes of VuSDGs and VuJMJs are labeled within boxes on the left, separated by light gray dotted lines, with colors corresponding to each specific class. Coding sequences (CDS), untranslated regions (UTRs), and introns are depicted as green rectangles, red rectangles, and black lines, respectively. The genes displayed were randomly selected to represent each class of VuSDGs and VuJMJs identified in the cowpea genome.

The VuSDG genes exhibited considerable structural diversity, with exon counts ranging from 1 to 26 and introns from 0 to 25 (Table S7; Figure 3A). Notably, *VuSDGVI.2* and *VuSDGVI.6*, both members of Class VI, contain no introns and consist of a single exon each. VuSDG gene structures encompass one to seven domains, with Classes I and IV showing

consistent domain counts of four and two, respectively, within their groups. Classes III (2–7 domains, 2–26 exons, and 1–25 introns) and VI (1–5 domains, 1–20 exons, and 0–19 introns) exhibit the greatest structural variability. In contrast, no variations in domain, exon, or intron counts were observed among members of Class IV.

For VuJMJ genes, exon counts range from 2 to 33, introns from 1 to 32, and domains from 1 to 5 (Table S8; Figure 3B). All VuJMJ genes contain at least one intron, with the Jmj-only, JMJD6, and KDM5 classes showing the highest variability—displaying intron counts ranging from 3 to 12, 1 to 15, and 11 to 32, respectively (Figure 3B). Despite some variability, gene structure conservation is generally observed within each class. For instance, the PKDM8 class has a conserved structure across all members, with each containing 11 exons, 10 introns, and three domains.

2.1.3. Gene Duplication Mechanisms of the VuSDGs and VuJMJs Loci

The analysis of gene duplication elucidated the mechanisms driving the expansion of VuSDGs and VuJMJs in the cowpea genome (Tables S9 and S10). Notably, members of neither VuSDGs nor VuJMJs expanded through proximal or tandem duplication mechanisms (Figure 4). Five VuSDG members belonging to classes VI and VII were identified as singletons (Figure 4A). Additionally, six VuSDG genes were found to have expanded via whole-genome duplication (WGD)/segmental duplication mechanism, resulting in three pairs of duplicated genes positioned into classes I, III, and V. The majority of VuSDGs—36 out of the 47 analyzed genes—exhibited dispersed duplication, which emerged as the predominant mechanism for VuSDG expansion within the cowpea genome.

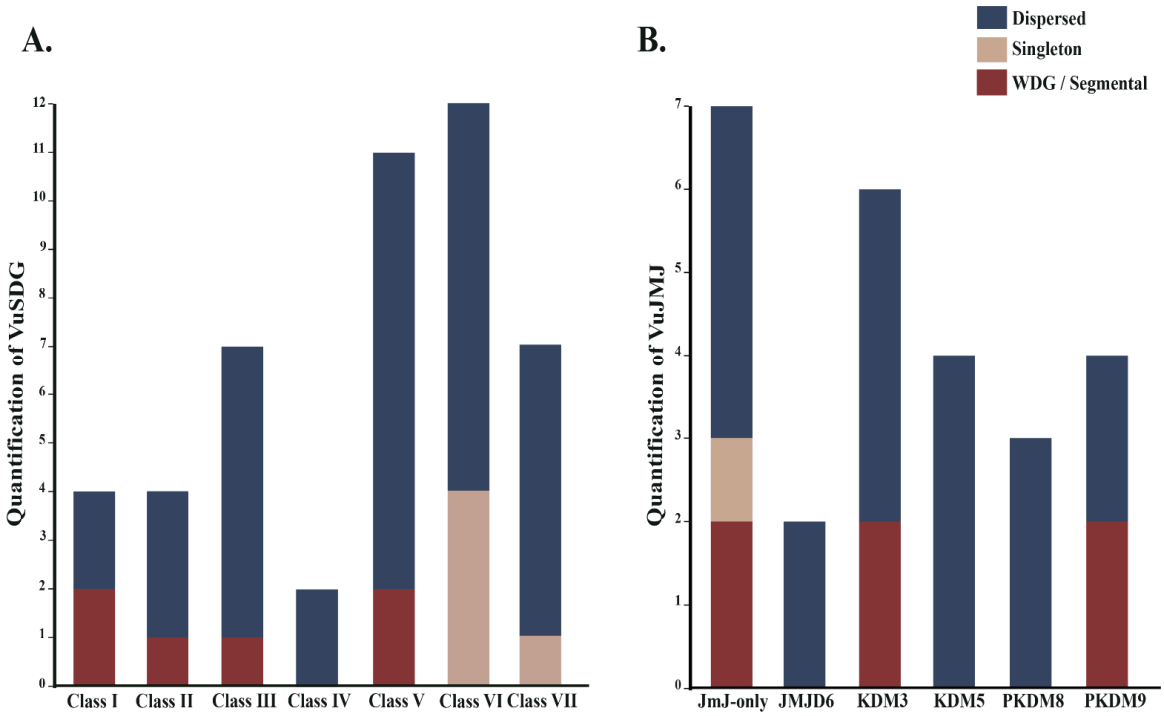


Figure 4. Quantification of the primary expansion mechanisms for the various classes/groups of VuSDG (**A**) and VuJMJ (**B**) genes identified in the cowpea genome. The *x*-axis represents the gene classes, and the *y*-axis shows the corresponding quantities for each class.

In contrast, only one VuJMJ gene, classified within the Jmj-only class, was identified as a singleton (Figure 4B). Six VuJMJ genes, resulting from WGD/segmental duplication, were found, forming three pairs of genes belonging to the Jmj-only, KDM3, and PKDM9

classes. Additionally, 19 VuJMJ genes were traced back to dispersed duplication, which also represents the primary mechanism of VuJMJ expansion within the cowpea genome.

2.1.4. Selection Pressure on Duplicated VuSDGs and VuJMJs Genes

The ratio of Ka/Ks was analyzed for the three pairs of duplicated genes resulting from WGD/segmental duplication in each gene family examined. The Ka/Ks values for VuSDGs ranged from 0.62 to 0.97, while those for VuJMJs varied between 0.46 and 0.96 (Table S11). All analyzed gene pairs of VuSDGs and VuJMJs exhibited Ka/Ks values less than 1, indicating that these genes are under purifying selection and suggesting a trend towards the conservation of amino acid sequences.

2.1.5. Orthology of VuSDGs and VuJMJs Genes in Viriplantae

An analysis of the orthology of VuSDGs and VuJMJs across different species of Viridiplantae was conducted, revealing that 64 out of 93 genomes examined contain orthologous loci corresponding to the VuSDGs and VuJMJs (Tables S12 and S13). The 20 species with the highest levels of orthology with cowpea are illustrated in Figure 5. Members of the Leguminosae family were prominent, displaying the highest levels of gene orthology, specifically *G. max* (96%), *P. vulgaris* (96%), *M. truncatula* (91%), and *Trifolium pratense* (91%). Furthermore, species from the Brassicaceae family, including *A. thaliana* (85%), *Brassica rapa* (85%), and *Eutrema salsugineum* (85%), exhibited significant levels of orthology with cowpea (Figure 5A). In the analysis of VuJMJs, 25 out of 26 loci in cowpea showed orthologs in the genomes of *P. vulgaris* (common bean) and *Daucus carota* (carrot), demonstrating approximately 96% conservation. Additionally, several Brassicaceae species, such as *Arabidopsis lyrata* (89%), *B. rapa* (89%), *Capsella grandiflora* (89%), *E. salsugineum* (89%), *Boechera stricta* (85%), and *Capsella rubella* (85%), presented orthologous JMJs to those in cowpea (Figure 5B).

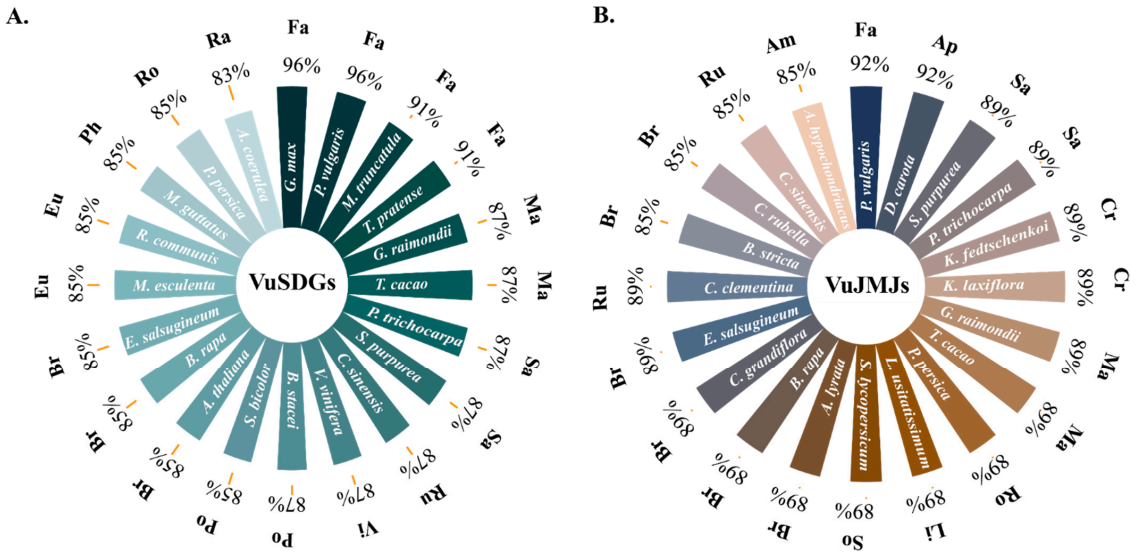


Figure 5. Quantification of conserved loci for histone methyltransferases (**A**) and histone demethylases (**B**) among the 20 plant species with the highest orthology indices relative to the VuSDGs and VuJMJs. The plant families are represented by letters adjacent to the bars as follows: Fa (Fabaceae), Ma (Malvaceae), As (Salicaceae), Ru (Rutaceae), Vi (Vitaceae), Po (Poaceae), Br (Brassicaceae), Eu (Euphorbiaceae), Ph (Phirmaceae), Ro (Rosaceae), Ra (Ranunculaceae), Ap (Apiaceae), Cr (Crassulaceae), Li (Linaceae), So (Solanaceae), and Am (Amaranthaceae). The analyzed species are indicated within the bars, each distinguished by different colors. The percentages of gene orthology for each analyzed species in relation to cowpea are presented above the bars.

2.1.6. CCREs in the Promoter Regions of the VuSDGs and VuJMJs Genes

All VuSDG- and VuJMJ-coding genes had their (1 Kb) predicted promoters analyzed for CCREs (Figure 6 and Table S14). For the promoters of VuSDGs, five CCREs were identified within the specified cutoff ($e < 10^{-2}$). These CCREs are associated with two distinct families of transcription factors (TFs): Dof-type (four motifs) and bZIP (one motif) (Figure 6). The CCREs linked to the Dof-type TF (JASPAR IDs MA1267.1, MA1268.1, MA1272.2, and MA1274.1) were the most abundant, appearing in 56 distinct sites.

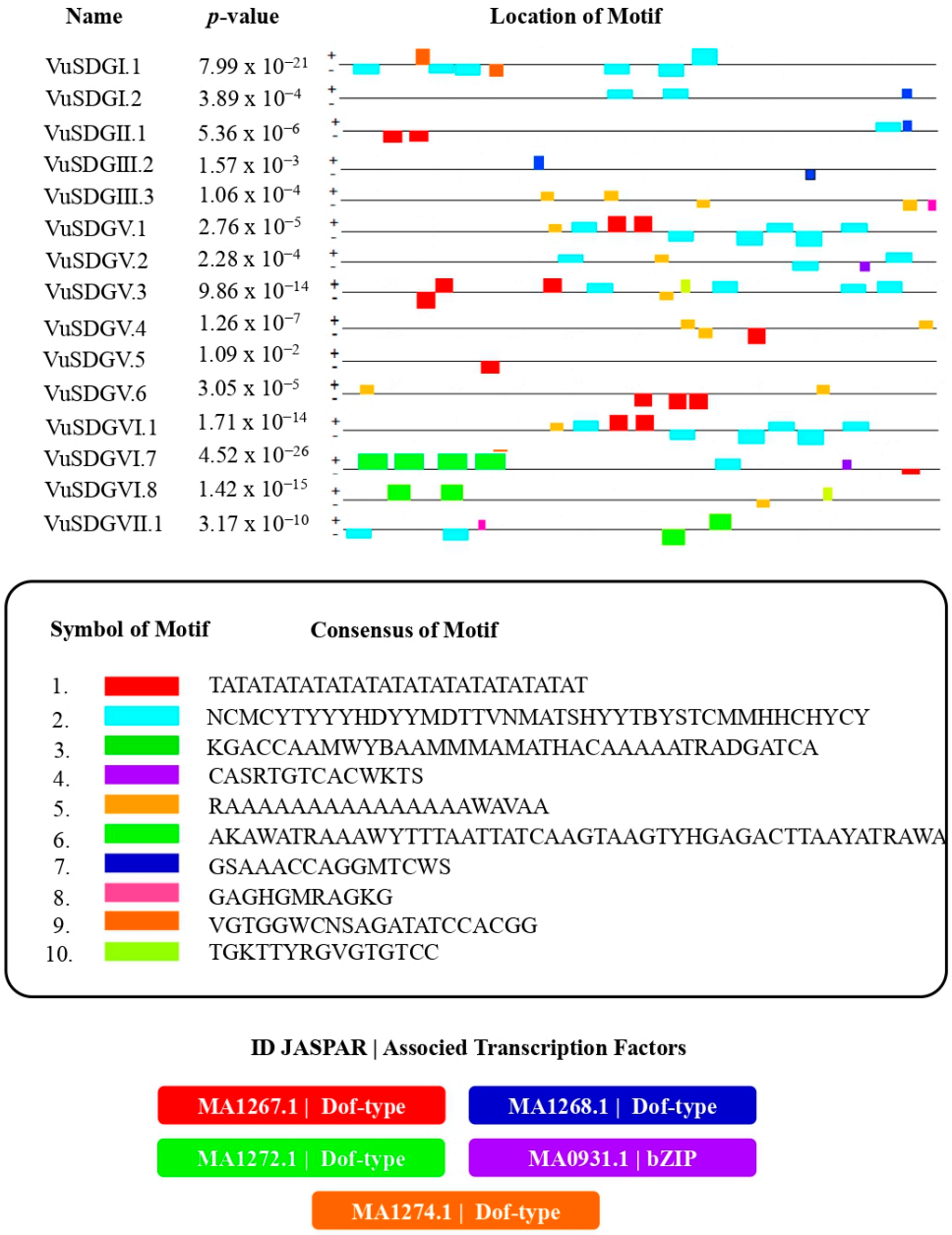


Figure 6. Localization and identification of CCREs, presentation of consensus motifs, and associated transcription factors in the promoters of a representative sample containing 15 VuSDG genes. The gene sample plotted was randomly selected to display all the CCREs identified within the total set of analyzed promoters. **Legend:** In the upper panel, each analyzed promoter displays the motifs in their entirety. The central panel presents the consensus of the motifs along with their respective symbols (colors). In the lower panel, bona fide CCREs are represented by rectangles of varying colors, illustrating their corresponding associated transcription factors.

In contrast, the promoters of VuJMJs contained only one CCRE within the stipulated cutoff, which was distributed across 21 distinct sites. This element was associated with the Dof-type TF (JASPAR ID 1278.1) (Figure 7).

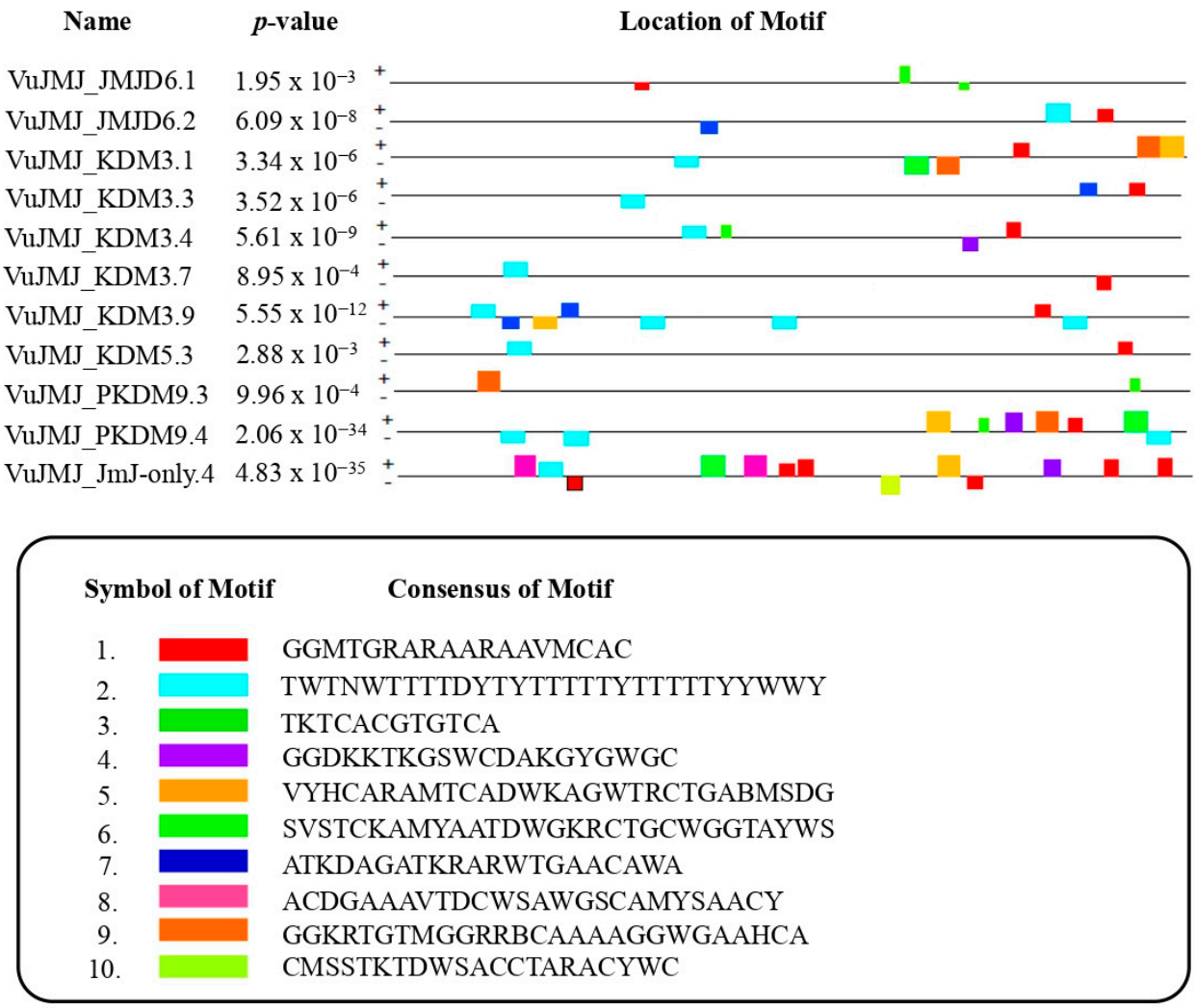


Figure 7. Localization and identification of CCREs, presentation of consensus motifs, and associated transcription factors in the promoters of a representative sample containing 11 VuJMJ genes. The genes plotted were randomly selected to display all the CCREs identified within the total set of analyzed promoters. **Legend**: In the upper panel, each analyzed promoter displays the motifs in their entirety. The central panel presents the consensus of the motifs along with their respective symbols (colors). In the lower panel, bona fide CCREs are represented by red rectangles, illustrating their corresponding associated transcription factor.

2.2. Transcriptomics of VuSDGs and VuJMJs in Cowpea Under Different Stresses

We investigated the expression patterns of VuSDG and VuJMJ transcripts using RNA-Seq data from cowpea plants exposed to three distinct stress conditions of strategic relevance: (a) mechanical injury followed by CABMV inoculation (analyzed in a resistant accession at 60 min and 16 h post-treatment); (b) mechanical injury followed by CPSMV inoculation (analyzed in a resistant accession at 60 min and 16 h post-treatment); and

(c) root dehydration (analyzed in a tolerant accession at 25 min and 150 min post-treatment). The complete transcriptomic data for VuSDG and VuJMJ expression profiles under these stress conditions are available in Supplementary Tables S15 and S16.

2.2.1. VuSDG and VuJMJ Expression Profiles in the Root Dehydration Assay

For the root dehydration (RD) assay, 330 transcripts encoding VuSDGs were retrieved and characterized. Among these, 26 unique VuSDG transcripts showed differential expression (Figure 8A), representing seven classes of histone methyltransferases (Classes I, II, III, IV, V, VI, and VII). Additionally, 134 VuJMJ transcripts were identified in the assays, with 17 unique VuJMJ transcripts displaying differential expression (Figure 8B), spanning five groups/subgroups of histone demethylases (Jmj-only, KDM3, KDM5, PKDM8, and PKDM9). Under the RD25 treatment, three VuSDG transcripts were upregulated, and 13 were downregulated (Table S15; Figure 8A). The upregulated transcripts belonged to Classes V and I, while the downregulated ones were distributed across Classes I, II, III, V, VI, and VII.

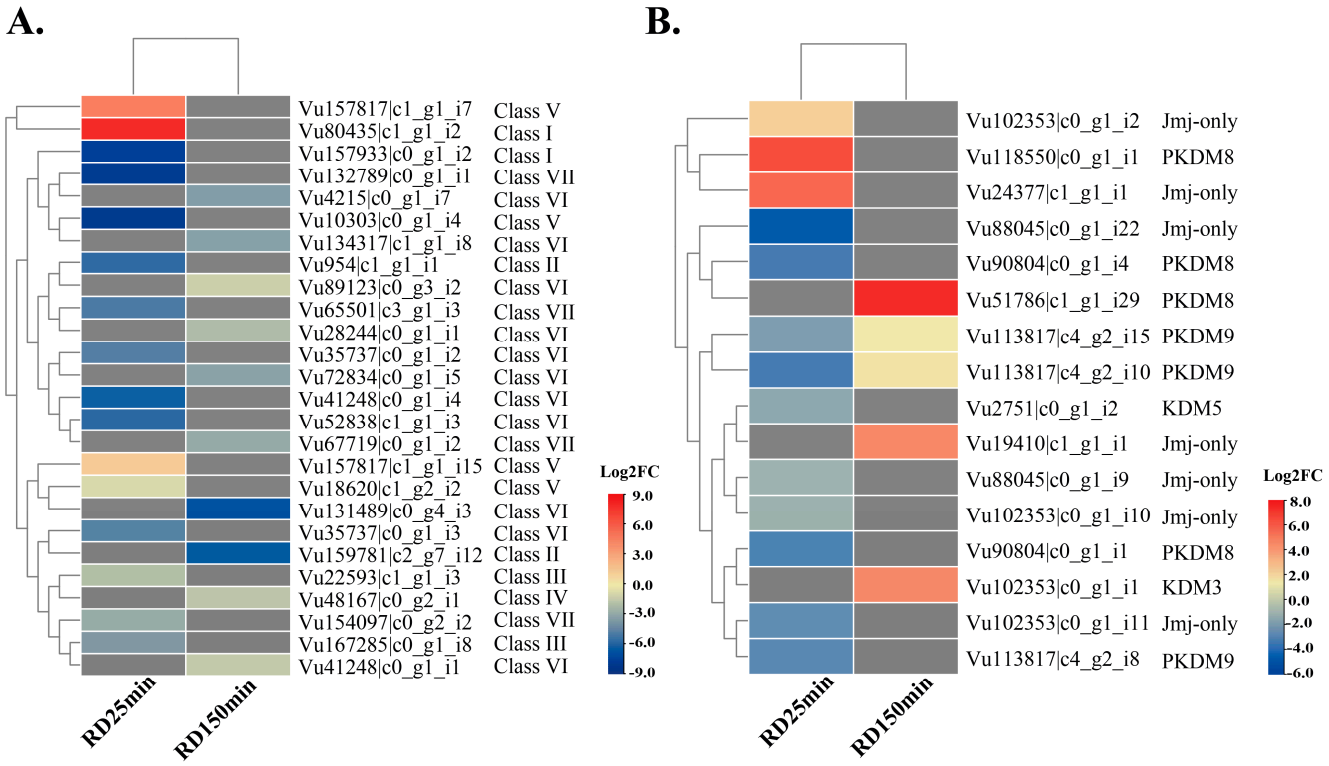


Figure 8. Heat map illustrating the modulation of transcripts encoding VuSDGs (**A**) and VuJMJs (**B**) that were differentially expressed in at least one treatment time point (RD25 or RD150) following root dehydration application.

For the RD150 treatment, all 10 differentially expressed VuSDG transcripts were downregulated, falling into Classes II, IV, VI, and VII (Table S15; Figure 8A).

Considering VuJMJs, the RD25 treatment revealed three upregulated transcripts and nine downregulated (Table S16; Figure 8B). The upregulated transcripts in this treatment were associated with the Jmj-only group and the PKDM8 subgroup, while the downregulated transcripts spanned the Jmj-only, PKDM8, PKDM9, KDM3, and KDM5 groups/subgroups (Table S16; Figure 8B).In the RD150 treatment, five VuJMJ transcripts were upregulated, representing the PKDM8, PKDM9, KDM3, and Jmj-only groups/subgroups (Table S16; Figure 8B). Notably, unlike VuSDGs, no downregulated VuJMJ transcripts were detected in the RD150 treatment (Table S16; Figure 8B). The PKDM8

and Jmj-only groups/subgroups consistently showed upregulated transcripts in both RD25 and RD150 treatments (Table S16). On the other hand, the PKDM9 and KDM3 groups/subgroups demonstrated a distinct temporal response, being exclusively upregulated in RD150 (Table S16; Figure 8B).

These findings suggest that as root dehydration stress persists, the tolerant cowpea accession reduces methylation activity on target histones and shifts towards demethylation action. This dynamic adjustment between histone methylation and demethylation may modulate the expression of genes associated with dehydration tolerance. The balance between the actions of VuSDGs and VuJMJs appears to be relevant for cowpeas' adaptation to low water availability, fine-tuning stress tolerance gene expression as the intensity and duration of stress increase.

2.2.2. VuSDG and VuJMJ Expression Profiles in the Mechanical Injury Followed by Virus Inoculation Assays

Transcripts encoding differentially expressed VuSDGs were absent at 16 h post-treatment in the mechanical injury followed by CABMV inoculation assay. However, at the 60 min post-treatment, one transcript was upregulated (class V), and one was downregulated (class VI) (Table S15). In the mechanical injury followed by CPSMV inoculation assay, three VuSDG transcripts showed differential expression. At 60 min post-treatment, one transcript was upregulated (class III), and another was downregulated (class VI). By 16 h post-treatment, only one VuSDG transcript was downregulated (class VII) (Table S15).

No VuJMJ transcripts were differentially expressed at 16 h post-treatment in the mechanical injury followed by CABMV inoculation assay. However, at 60 min post-treatment, four VuJMJ transcripts from the Jmj-only group were upregulated (Table S16). In the analogous mechanical injury and CPSMV inoculation assay, two VuJMJ transcripts exhibited differential expression at 60 min post-treatment, with one transcript upregulated (PKDM8 subgroup) and one downregulated (PKDM9 subgroup) (Table S16). At 16 h post-treatment, a single Jmj-only transcript was downregulated (Table S16). The results mentioned above indicated that in the mechanical injury followed by virus inoculation assays, VuSDGs and VuJMJs exhibited similar transcriptional modulation. The main point of divergence was the predominant upregulation of VuJMJs at 60 min post-treatment in the mechanical injury followed by the CABMV inoculation assay.

2.2.3. VuSDG and VuJMJ Crosstalk Response Investigation

The upregulated VuSDG transcripts were unique to each assay, with no overlapping (crosstalk) transcripts identified between them. In contrast, within the VuJMJ family, one transcript from the PKDM8 subgroup was upregulated in both the "mechanical injury followed by CABMV inoculation" and "root dehydration" assays, indicating its possible role in cowpea's response to diverse stress conditions (Tables S15 and S16).

2.3. RNA-Seq Data Validation Through qPCR Assay

To assess the reliability and robustness of in silico gene expression (RNA-Seq libraries), differentially expressed VuSDG and VuJMJ transcripts were further analyzed through qPCR. Following standard primer design criteria, 15 primer pairs were designed for these transcripts: seven pairs targeting VuSDG transcripts and eight for VuJMJ transcripts (Table S17). The primer pairs covered all investigated assays. Specificity was confirmed by the presence of a single peak in the melting curves (Supplementary Appendix S1).

For the VuSDG primers, only two pairs demonstrated acceptable amplification efficiencies (90–110%), with efficiencies of 95.2% and 101.5%, targeting the transcripts Vu90804 | c0_g1_i1 and Vu72834 | c0_g1_i5, respectively (Table S17). Both transcripts were downregulated in the root dehydration assay (Supplementary Appendix S2). Functional

primer pairs for VuSDG transcripts in the mechanical injury followed by viral inoculation assays could not be obtained.

For the VuJMJ transcripts (Vu2751 | c0_g1_i2, Vu102353 | c0_g1_i11, Vu88045 | c0_g1_i9, Vu102353 | c0_g1_i2, Vu167285 | c0_g1_i8, Vu19410 | c1_g1_i1, Vu113817 | c4_g2_i10, and Vu113817 | c4_g2_i3), all primer pairs exhibited acceptable efficiencies, ranging from 93.3% to 108.1% (Table S17). This set of primer pairs covered all conducted assays.

Relative expression qPCR analysis indicated that both VuSDG transcripts were downregulated in the root dehydration assay: Vu72834 | c0_g1_i5 in the RD25 treatment, and Vu90804 | c0_g1_i1 in the RD150 treatment, corroborating the RNA-Seq data (Figure 9).

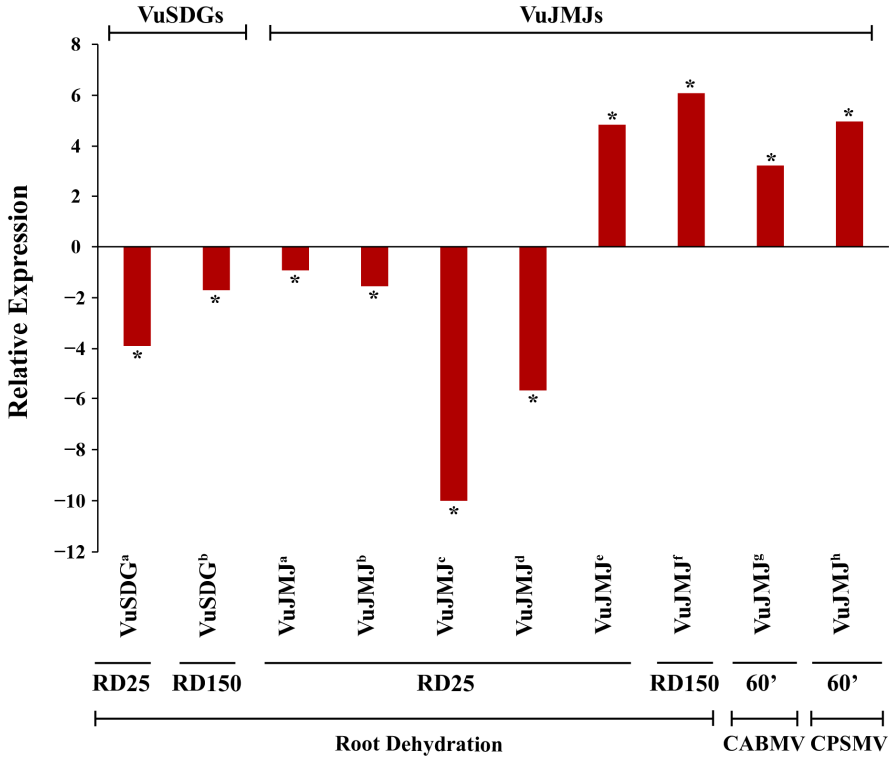


Figure 9. Relative expression of differentially expressed VuSDG and VuJMJ transcripts as determined via qPCR. **Legend:** The asterisk (*) indicates differentially expressed transcripts with $p < 0.05$. Transcript identifiers are listed vertically below the bars as follows: VuSDG[b] (Vu167285 | c0_g1_i8); VuJMJ[a] (Vu90804 | c0_g1_i1); VuJMJ[b] (Vu2751 | c0_g1_i2); VuJMJ[c] (Vu102353 | c0_g1_i11); VuJMJ[d] (Vu88045 | c0_g1_i9); VuJMJ[e] (Vu102353 | c0_g1_i2); VuJMJ[f] (Vu19410 | c1_g1_i1); VuJMJ[g] (Vu113817 | c4_g2_i10); VuJMJ[h] (Vu113817 | c4_g2_i3).

For the VuJMJ transcripts, the qPCR assay indicated that in the mechanical injury followed by viral inoculation assay, two transcripts were upregulated: Vu113817 | c4_g2_i10 in response to CABMV and Vu113817 | c4_g2_i3 in response to CPSMV, both at 60 min post-treatment. In the root dehydration assay, transcripts Vu90804 | c0_g1_i1, Vu2751 | c0_g1_i2, Vu102353 | c0_g1_i11, and Vu88045 | c0_g1_i9 were downregulated under the RD25 treatment, while transcripts Vu113817 | c4_g2_i10 and Vu113817 | c4_g2_i3 were upregulated under RD25 and RD150, respectively (Figure 9). All these qPCR results were consistent with the RNA-Seq data.

In summary, 15 primer pairs were designed for the differentially expressed VuSDG and VuJMJ transcripts identified in the RNA-Seq libraries. Of these, 10 primer pairs were functional, demonstrating acceptable efficiency values. All functional primer pairs validated via qPCR (Supplementary Appendix S2) corroborated the RNA-Seq results, underscoring the robustness of the RNA-Seq dataset.

3. Discussion

3.1. Mining and Gene Structural Characterization of VuSDGs and VuJMJs in the Cowpea Genome

The identification of SDG and JMJ gene families has been widely reported across plant species; however, for cowpea—a species of strategic importance—a considerable information gap remained. In this study, 47 VuSDG and 23 VuJMJ genes were identified. Similar counts have been reported for *A. thaliana* (47 SDG and 21 JMJ genes) [5,31], rice (43 SDG and 20 JMJ) [19,31], and maize (43 SDG and 19 JMJ) [15,21]. Among legumes, data were limited to the JMJ family in soybean, which comprises 48 genes [23]. The variability in JMJ gene numbers may be linked to the broad range of genome sizes across species. Cowpea has a genome size of 640 Mb (2n = 2x = 22) [30], whereas soybean, a tetraploid species (2n = 4x = 40), has a genome of approximately 1.15 Gb [32]. In hexaploid wheat, with 2n = 6x = 42 and a genome size of ~16 Gb [33], 166 SDG genes have been identified.

The highly conserved SET domain in VuSDG proteins is essential for the catalytic activity of histone methyltransferases [19]. Beyond this entity, VuSDG proteins harbor additional domains, including AWS, WIYLD, Pre-SET, PHD, PWWP, FYRC, FYRN, Post-SET, Zf-CW, CXC, and SANT. Most of these domains are involved in DNA binding and contribute to the functional specificity of the proteins. The identification of these elements, combined with phenetic analysis, facilitated the classification of VuSDG proteins into seven distinct classes, aligning with classifications previously reported in *A. thaliana* [5] and *Dendrobium catenatum* [34].

All VuJMJ proteins contained a conserved JmjC domain, a hallmark of the JMJ gene family, which is associated with the demethylation of lysine residues in histones [16]. Additional domains, such as zf-4CXXC_R1, Zf-C5HC2, FYRN, and FYRC, were also identified and are known to play roles in DNA binding. The VuJMJs were categorized into six groups/subgroups: JmjC-only (represented by PKDM11-12-13 in soybean) [23], JMJD6, KDM3, KDM5, and PKDM8–9 (corresponding to the KDM4 group in *A. thaliana*, rice, and cotton) [16,31]. Notably, the abundance of class V and KDM3 members in cowpea and their established roles in silencing transposable elements (TEs) and repetitive DNA regions [35] highlight these classes as promising targets for future physiological studies in this species.

This study analyzed gene structure diversity, focusing on exon and intron gain or loss among elements within the studied families. Inter-group/class variation in intron number was observed, though intra-group/class conservation was maintained. This inter-group/class variation in intron count may reflect specific selective and adaptive pressures unique to each group/class, potentially contributing to the versatility and functional specialization of genes within these families.

3.2. Protein Properties and Prediction of Subcellular Localization

Subcellular localization analysis showed that VuSDG and VuJMJ proteins were predominantly localized in the nucleus, consistent with their roles in catalyzing histone (de)methylation within the nucleus. However, some VuSDG and VuJMJ members were also predicted to localize in the chloroplast, cytoplasm, plasma membrane, and mitochondria. Similar observations have been reported for *B. rapa* [14]. SDG proteins with non-histone methylation activity, particularly those with truncated SET domains, have been identified [5], such as the class VII proteins in this study. These findings emphasize the functional versatility of these proteins in cowpea, suggesting their potential activity across multiple cellular compartments.

3.3. Duplication Mechanisms of VuSDG and VuJMJ Genes in the Cowpea Genome

Gene duplication is a key mechanism in plant species evolution [25], contributing to the expansion of gene families and the emergence of novel biological functions. In the

case of the VuSDG and VuJMJ gene families, dispersed duplication and WGD/segmental duplications were the main drivers of expansion, with dispersed duplication being the predominant force. Similar findings have been reported for JMJ genes in *Fragaria vesca* [36], suggesting that this type of duplication plays a significant role in JMJ gene expansion in plants. Genes duplicated through this mechanism may have originated from the activity of transposable elements (TEs), as observed in various organisms [37]. In higher plants, genomes often contain a high proportion of TEs. For instance, species such as *Vigna angularis*, *Vigna radiata*, and cowpea exhibit 43%, 50%, and 50.1% repetitive sequences in their genomes, with approximately 32%, 39%, and 39%, respectively, corresponding to TEs [30,38]. The Ka/Ks ratio, which serves as an indicator of selective pressures on gene sequences, was analyzed for the VuSDGs and VuJMJs that underwent WGD/segmental duplication. All VuSDG and VuJMJ gene pairs had a Ka/Ks ratio < 1, suggesting that these genes are under purifying selection. This type of selection promotes the conservation of amino acid sequences, preserving both their functionality and structure. These findings imply that the gene pairs may exhibit functional redundancy, highlighting their essential roles in cellular processes.

3.4. Comparative Genomics of VuSDGs and VuJMJs

A high degree of homology was observed for VuSDGs and VuJMJs across the analyzed genomes, indicating substantial conservation of these genes. As expected, legume species—especially common bean and soybean—showed the highest orthology indices with cowpea. These findings pave the way for functional studies on these conserved proteins in related species.

3.5. Mining and Identification of Candidate CCREs

The CCREs identified in our study may provide insights into the potential roles of VuSDGs and VuJMJs by linking them to associated transcription factors (TFs) and their respective biological processes. Specifically, Dof-type and bZIP TFs, which are associated with the bona fide CCREs of VuSDGs and VuJMJs, are involved in stress responses in plants. Dof-type TFs, for example, play a role in responses to pathogenic agents such as viruses and fungi [39,40]. In contrast, bZIPs are a plant-specific TF family crucial for mediating responses to both biotic stresses, such as *Sclerotinia sclerotiorum*, a necrotrophic phytopathogen common to soybean [41], and abiotic stresses like drought [42]. The CCREs identified in the promoters of cowpea VuSDG and VuJMJ genes suggest that histone methyltransferases and demethylases may be involved in a variety of processes in cowpea, thus enhancing its biotechnological potential.

3.6. Transcriptomics of VuSDGs and VuJMJs in Cowpea Under Biotic and Abiotic Stress

The qPCR analysis validated the RNA-Seq expression results for a sample of 10 tested targets (two VuSDGs and eight VuJMJs), reinforcing the reliability of the RNA-Seq library preparation and the statistical methods employed. This validation underscored the robustness of the transcriptomic findings presented in this study.

The global expression profile of VuSDGs in response to root dehydration revealed transcripts (from classes V and I) that were exclusively upregulated under the RD25 treatment. In contrast, for VuJMJs, upregulated transcripts—including those from the Jmj-only, KDM3, and PKDM8–9 groups/subgroups—were observed under both RD25 and RD150 treatments. Notably, transcripts upregulated in RD150 were exclusively associated with the VuJMJ family, specifically within the PKDM8–9, Jmj-only, and KDM3 groups/subgroups. These findings suggest that, as root dehydration stress progresses, the tolerant cowpea accession reduces methylation activity on target histones and shifts towards demethylation. The demethylation of H3K27me, catalyzed by KDM3, is known to be an important drought

response in plants. In Arabidopsis, the reduction in H3K27me3 levels in intergenic regions of NAC family transcription factors, which respond to drought stress via ABA hormone perception, significantly contributes to drought tolerance [43]. Thus, it is proposed that KDM3 may play a similar role in activating genes involved in hormonal perception and drought stress response in cowpeas under root dehydration. Other studies also indicate the critical roles of VuSDG and VuJMJ genes in drought tolerance across various plant species [27,34].

Despite their recognized importance in response to biotic stresses, studies on the role of the SDG and JMJ gene families in plant defense have been primarily focused on bacteria (e.g., *Pseudomonas syringae* pv tomato DC3000 [44]) and fungi (e.g., *Uromyces appendiculatus* [45] and *Botrytis cinerea* [46]). Notably, information regarding their role in defense against viruses has been lacking. Our RNA-Seq data indicated a modest yet discernible involvement of VuSDGs and VuJMJs in cowpeas' response to mechanical injury followed by virus inoculation within the specified timeframe. Specifically, only one VuSDG transcript (Class V) was upregulated 60 min post-treatment in each respective assay. For VuJMJs, four transcripts (Jmj-only group) were upregulated in the CABMV assay, and one (PKDM8 group) in the CPSMV assay, all at the 60-min post-treatment mark. No up-regulation of VuSDG or VuJMJ transcripts was observed at 16 h post-treatment in either assay.

These findings suggest a potential early role for some VuJMJ and VuSDG elements in cowpea's defense response to injury followed by virus inoculation. Additionally, considering different VuSDGs classes and VuJMJs groups, Class V (VuSDGs) and the PKDM8 and Jmj-only groups (VuJMJs) are particularly notable for their upregulation across two distinct assays (root dehydration and mechanical injury followed by CABMV inoculation). Members of class V and PKDM8 catalyze the methylation and demethylation of H3K9me, respectively [5,32]. On the other hand, the Jmj-only class is associated with the demethylation of H3K27me [47]. The H3K9me modulates defense-related genes in common bean under *Uromyces appendiculatus* attack [45]. In wheat, the *TaSDG20-3D* (class V) gene has been reported to participate in defense responses against multiple stresses, including water deficit stress, heat, and resistance to leaf rust caused by *Puccinia recondita* [27]. In Arabidopsis, the demethylation of the H3K9me mark mediated by the JMJ27 gene is directly linked to the regulation of the drought stress response [48].

4. Materials and Methods

4.1. Genomic Section

4.1.1. Mining and Identification of VuSDG and VuJMJ Coding Loci

Protein sequences with SET (PF00856) and JmjC (PF02373) domains, associated with histone methyltransferase and demethylase families, respectively, were retrieved from the GenBank "https://www.ncbi.nlm.nih.gov/genbank/ (accessed on 4 September 2024)" and UniProt "https://www.uniprot.org/ (accessed on 4 September 2024)" databases. These sequences, originating from *A. thaliana*, rice, maize, and *Medicago truncatula*, were used to identify (through similarity analyses) VuSDG and VuJMJ loci in the cowpea genome (Materials S1 and S2).

Protein alignments were conducted against the cowpea conceptual proteome (Vunguiculata_469_v2.1.protein_primaryTranscriptOnly.fa, obtained from the Phytozome database) using BLASTp with an e-value threshold of $<e^{-10}$. For each cowpea gene, only the primary transcript's longest peptide sequence was retained, and Phytozome identifiers were linked to the corresponding loci.

To confirm the presence of conserved domains in candidate VuSDG and VuJMJ genes, Pfam "pfam.xfam.org/ (accessed on 11 September 2024)", the Conserved Domain Database

"https://www.ncbi.nlm.nih.gov/cdd/ ((accessed on 13 September 2024)", and SMART "smart.embl-heidelberg.de/ (accessed on 14 September 2024)" were used. A similar methodology was applied to identify VuSDGs and VuJMJs in CpG RNA-Seq libraries using tBLASTn (e-value < e^{-5}).

4.1.2. Classification of VuSDG and VuJMJ Genes

The studied genes were classified using two complementary strategies:

1. Profiling (presence/absence) of different domains to each VuSDG or VuJMJ class/group;
2. Conducting phenetic analysis of curated protein sequences from various species, focusing on SDG and JMJ sequences. Candidate VuSDGs and VuJMJs were aligned using ClustalW [49], and a phenetic tree was constructed with the Neighbor-Joining (NJ) method [50] in MEGA 7 [51], employing 1000 bootstrap replicates. Genes were categorized based on established classifications in *Arabidopsis thaliana* and rice, as well as the tree topology.

This dual characterization approach allowed for data validation when the two methods yielded convergent results. In cases of discrepancies between the two strategies, precedence was given to the domain profiling results, as this approach focuses on the functional structure of the molecular entities under investigation.

4.1.3. Structural Characteristics of VuSDG and VuJMJ Genes

GeneStats "https://gist.github.com/darencard/fcb32168c243b92734e85c5f8b59a1c3 (accessed on 23 September 2024)" was used to analyze gene structural features, including (1) transcript length; (2) exon count; (3) total exon length; (4) intron count; (5) total intron length; (6) CDS count; (7) CDS length; (8) 5′ UTR count; (9) 5′ UTR length; (10) 3′ UTR count; and (11) 3′ UTR length. Domain annotations for analyzed families were based on Pfam, the Conserved Domain Database, and SMART (2.1.1). Gene structures were visualized using the Gene Structure Display Server (GSDS 2.0) "https://gsds.cbi.pku.edu.cn (accessed on 25 September 2024)" [52].

4.1.4. Protein Properties and Subcellular Localization Prediction

The molecular weight (MW) and isoelectric point (pI) of all VuSDG and VuJMJ proteins were predicted using JVir Gel 2.0 [53]. CELLO 2.5 software [54] was used to predict subcellular localization.

4.1.5. Expansion Mechanisms of VuSDG and VuJMJ Genes

Gene family expansion mechanisms were assessed with MCScanX software (https://github.com/wyp1125/MCScanX accessed on 28 September 2024) [55], classifying them as dispersed, tandem, proximal, and segmental (WGD/segmental) duplications. Genes without duplicates were identified as singletons. Duplication classification followed the criteria outlined by Wang et al. [55].

4.1.6. Synonymous (Ks) and Non-Synonymous (Ka) Substitution Rates for WGD/Segmental Duplicated Genes

Selective pressure on WGD/segmental duplications was evaluated using Ka/Ks ratios. Complete coding sequences of WGD/segmental duplicated VuSDGs or VuJMJs were independently aligned with ClustalW 2.0 [49], and Ka and Ks rates were calculated via the Jukes–Cantor model in MEGA 7 [51]. Ka/Ks values serve as indicators of selective pressure. Values below "1" suggest purifying selection, where sequence conservation is favored; values equal to "1" imply neutral selection, and values above "1" indicate positive selection, leading to sequence divergence.

4.1.7. Orthology Analysis of VuSDG and VuJMJ Loci Across Viridiplantae Species

Orthologous analysis was performed using the Phytozome database "https://phytozome.jgi.doe.gov/pz/portal.html (accessed on 28 September 2024)" and the PhytoMine tool (InterMine-based), comparing the genes against 93 genomes from 82 Viridiplantae species. InParanoid 8 software [56] was used to generate orthologous relationships.

4.1.8. Candidate Cis-Regulatory Element (CCRE) Mining and Identification

Promoter sequences (1 Kb) for VuSDG and VuJMJ genes were obtained from Phytozome v.12.1.6 through the Phytozome API (Application Programming Interface). CCREs were searched using MEME v5.0.3 "https://meme-suite.org/tools/meme (accessed on 4 October 2024)" [57] in classic mode, set to identify up to ten motifs with lengths between 6 and 50 nucleotides and e-values < 10^{-2}. Transcription factors (TFs) potentially binding to CCREs were identified using TomTom v4.11.2 "https://meme-suite.org/tools/tomtom (accessed on 4 October 2024" [58] in conjunction with the JASPAR database (JASPAR2018_CORE_plants_non-redundant), which contains experimentally validated TF binding profiles. The resulting alignments were evaluated using *p*-values (<10^{-2}) and *q*-values (false discovery rate, FDR < 10^{-2}), with TF identities assigned based on the best alignment score.

4.2. Transcriptomics

4.2.1. Biological Material, Experimental Design, and Stress Application

Root Dehydration Assay

Seeds of *V. unguiculata* cv. Pingo de Ouro, a drought- and water-deficit-tolerant cultivar [59,60], were treated with Thiram (tetramethylthiuram disulfide) at a concentration of 0.05% (*w*/*w*). The seeds were germinated for two days under controlled conditions (temperature: 25 ± 1 °C, relative humidity: 65 ± 5%). Following germination, seedlings were transferred to a hydroponic system [61] containing an aerated, balanced nutrient solution at pH 6.6 [62]. The seedlings were secured to ensure complete root immersion in the hydroponic solution. Cultivation continued for three weeks in a greenhouse under natural photoperiods (approximately 13/11 h light/dark cycle), with environmental conditions maintained at a temperature of 30 ± 5 °C and relative humidity of 60 ± 10%. After the mentioned timeframe, root dehydration treatment was initiated by removing the nutrient solution from the treated plants. Root tissue samples were collected at 25 min (RD25) and 150 min (RD150) after solution removal, rapidly frozen in liquid nitrogen, and stored at −80 °C for subsequent RNA extraction. For each treatment duration, corresponding control groups (Cont.25 and Cont.150) were kept in the nutrient solution until collection. An experimental design (cultivar vs. root dehydration duration) with three biological replicates (BRs) per condition was employed, where each BR included two individual plants.

Cowpea seeds for the 'Pingo de Ouro' genotype (ID: Pingo_de_Ouro_1_2) were obtained from the Active Germplasm Bank of Cowpea at the Agronomic Institute of Pernambuco (IPA, Recife, PE, Brazil). Species/genotype identification was conducted by Prof. Dr. Antônio Félix da Costa (IPA).

Mechanical Injury and Viral Inoculation Assays

The experiments involved applying mechanical injury followed by inoculation with either CABMV (*Cowpea aphid-borne mosaic virus*) or CPSMV (*Cowpea severe mosaic virus*) under controlled greenhouse conditions at IPA. For the CABMV assay, we used the resistant cowpea genotype IT85F-2687 [63,64], while the CPSMV assay employed the resistant cowpea genotype BR-14 Mulato [65]. Both assays were conducted separately but followed the same experimental protocol and design.

Seeds of each accession were sown and cultivated for 21 days under natural photoperiod and temperatures ranging from 28 to 32 °C. Prior to virus inoculation, the youngest trifoliate leaves were mechanically abraded with carborundum (silicon carbide) to facilitate viral entry. The viral inoculum was then applied to each genotype. Negative controls, which received no mechanical injury or viral inoculation, were included for the combined stresses.

Leaf tissue samples were collected at two time points after the mechanical injury and viral inoculation treatments: 60 min post-treatment and 16 h post-treatment. At each collection time, leaf tissue from treated and control plants was immediately harvested, flash-frozen in liquid nitrogen, and stored at −80 °C until total RNA extraction. The experiment was performed with three biological replicates per condition, each consisting of five plants. To prevent potential interference from volatile compounds involved in interplant communication, treatments were conducted in isolated areas.

Seeds for the cowpea genotypes 'IT85F-2687' and 'BR-14 Mulato' were formally acquired from the 'Active Germplasm Bank of Cowpea' at IPA, with species/genotype identification confirmed by Prof. Dr. Antônio Félix da Costa (IPA). Differential gene expression in both presented assays reflected responses to dual stressors: mechanical injury and viral inoculation. Plant viruses are unable to initiate infection without initial mechanical damage, which may occur naturally via vector organisms or agricultural practices. Unlike bacteriophages and animal viruses, plant viruses lack specific cellular receptors [66]. Consequently, the combination of 'mechanical injury and viral inoculation' aims to simulate the infection process within a natural ecological context.

4.2.2. RNA-Seq Libraries: Synthesis and Sequencing

Total RNA was isolated using the 'SV Total RNA Isolation System' kit (Promega, Madison, WI, USA) following the manufacturer's protocol. The RNA concentration and quality were assessed using a NanoDrop spectrophotometer, 1.5% agarose gel electrophoresis, and the 'Agilent 2100 Bioanalyzer' (Agilent Technologies, Santa Clara, CA, USA). Only samples with an RNA integrity number (RIN) $\geq$ 8.0 were selected for sequencing. For mRNA purification and complementary DNA (cDNA) library construction, we used the 'TruSeq® Stranded mRNA LT-Set A' kit (RS-122-2101, Illumina, San Diego, CA, USA) in accordance with the manufacturer's guidelines. Paired-end reads, each 100 bp in length, were generated on an Illumina HiSeq 2500 system using the 'HiSeq® Rapid PE Cluster Kit v2' (PE-402-4002), 'SBS Kit v2' (200 Cycle; FC-402-4021), and the 'TruSeq® Stranded mRNA LT—Set A' (RS-122-2101). Transcriptome sequencing for the three cowpea genotypes was conducted at the Functional Genomics Center of the University of São Paulo (Piracicaba, SP, Brazil).

4.2.3. RNA-Seq Library Assembly and Differential Expression Analysis

The RNA-Seq libraries generated from the different assays were assembled using the pipeline described by Ferreira-Neto et al. [67]. Differential expression analysis was also conducted through the referred pipeline, applying the following criteria: $\log_2$ fold change ($\log_2$FC) thresholds of $-1 > \log_2\text{FC} > 1$, with p-values < 0.05 and false discovery rates (FDR) < 0.05.

4.2.4. qPCR: Setup, Efficiency, and Relative Expression Analyses

To validate the precision of RNA-Seq data, differentially expressed VuSDGs and VuJMJs transcripts were further analyzed via Quantitative Real-Time PCR (qPCR). Each sample included three biological replicates and three technical replicates to ensure statistical robustness. Primers were designed using Primer3 "https://bioinfo.ut.ee/primer3-0.4.0/ (accessed on 21 October 2024)" with the following specific settings: annealing temperature of 57–63 °C (optimum 60 °C), primer length of 18–22 bp (optimum 20 bp), GC content of 45–55% (optimum 50%), and an amplicon length of 100–200 bp. In total, 15 primer pairs

were designed—seven for VuSDG transcripts and eight for VuJMJ transcripts (Table S17). qPCR reactions were conducted on 96-well plates using a LineGene 9660 thermocycler (Bioer) with SYBR Green detection.

Aliquots of the same total RNA samples sent for RNA-Seq were used, with RNase-free DNase I treatment to remove any genomic DNA contamination. RNA concentration and quality were assessed using a NanoDrop 2000c spectrophotometer (ThermoFisher Scientific, Waltham, MA, USA) and 1% agarose gel electrophoresis stained with Blue Green (LGC, São Paulo, Brazil). For each sample, 1 μg of total RNA was reverse-transcribed into cDNA using the GoScript™ Reverse Transcription System (Promega) and oligo(dT) primers, following the manufacturer's protocol. The qPCR setup, PCR cycling, amplification efficiency, and melting curve analysis followed protocols outlined by [68].

Amplification efficiency ($E = 10^{(-1/\text{slope of the standard curve})}$) for all primer pairs was calculated using a four-point standard curve with serial 10× dilutions of cDNA in technical triplicates. Standard curve slopes in the range of −3.58 to −3.10 were accepted for the assay, correlating with amplification efficiencies between 90% (E = 1.9) and 110% (E = 2.1).

For normalization, Actin and Ubiquitin-Conjugating Enzyme E2 Variant 1D were chosen as reference genes for root dehydration data, following validations by Amorim et al. [68] in similar cultivar, tissue, and conditions. For mechanical injury followed by virus inoculation data, F-box protein and Ubiquitin 10 were used as reference genes, selected based on internal group data under matching conditions.

Relative expression levels of target transcripts were analyzed using REST2009 software (standard mode), which applies pairwise comparisons between target and reference genes under treated and control conditions via randomization and bootstrapping techniques—Pairwise Fixed Reallocation Randomization Test© (REST, 2009) [69]. Hypothesis testing ($p < 0.05$) determined the statistical significance of expression differences between control and treated conditions.

5. Conclusions

This study provides a comprehensive genomic and transcriptomic characterization of the SDG and JMJ gene families in cowpea. The findings not only enhance our understanding of the diversity and evolution of these gene families in leguminous plants but also offer new perspectives on their roles in other plant systems.

The VuSDG and VuJMJ genes, classified into seven and six distinct classes/groups, respectively, exhibited substantial variation in gene structure across the different groups and classes. Despite this diversity, there was considerable intra-class or intra-group conservation, suggesting that these gene families fulfill essential functions within the plant. The analysis of gene duplications, particularly the dispersed and WGD/segmental types, indicated that these mechanisms play a pivotal role in the expansion of these families in cowpea. The predominance of dispersed duplication as the primary mechanism of expansion supports the notion that random duplication events may influence adaptation and the functionality of the encoded proteins.

The identification of CCREs, in conjunction with transcriptomic analysis, suggested that the VuSDG and VuJMJ genes play crucial roles in cowpeas' response to a variety of environmental stresses. The capacity of these gene families to respond to both abiotic stresses, such as root dehydration, and biotic stresses, as demonstrated in assays with CABMV and CPSMV, underscores their role in maintaining cellular homeostasis and defending against pathogens. The differential expression of VuSDG and VuJMJ genes also implies that these families may be involved in early signaling mechanisms and the modulation of defense pathways, which are essential for the plant's survival in challenging environments.

The insights gained from this study position VuSDG and VuJMJ genes as promising targets for biotechnological interventions, including gene editing, transgenesis, and molec-

ular breeding approaches aimed at enhancing cowpea and other legume production in stress-prone environments.

Supplementary Materials: The following supporting information can be downloaded at: https://www.mdpi.com/article/10.3390/stresses5010013/s1, Material S1. Sequences containing the characteristic domains of histone methyltransferases used as probe sequences to identify SDG candidates in the cowpea genome. Material S2. Sequences containing the characteristic domains of histone demethylases used as probe sequences to identify JMJ candidates in the cowpea genome. Supplementary Appendix S1. Melting curves for target transcripts used in the present study. Supplementary Appendix S2. REST software outputs for target transcripts relative expression assay. Table S1. SDG genes identified in the cowpea genome, presenting their respective IDs, classes, and conserved domains. Table S2. Characterization of VuSDGs regarding nucleotide length, polypeptide chain length, isoelectric point (pI), molecular weight (MW), and subcellular localization. Table S3. JMJ genes identified in the cowpea genome, including their respective IDs, classes, and conserved domains. Table S4. Characterization of VuJMJs regarding their nucleotide length, polypeptide chain length, isoelectric point (pI), molecular weight (MW), and subcellular localization. Table S5. Chromosomal localization of SDG genes identified in the cowpea genome. Table S6. Chromosomal localization of JMJ genes identified in the cowpea genome. Table S7. Structural characterization of VuSDG genes, indicating the ID of each locus and 12 parameters defining their respective gene structures. Table S8. Structural characterization of VuJMJ genes, indicating the ID of each locus and 12 parameters defining their respective gene structures. Table S9. Duplication mechanisms of VuSDG genes. Table S10. Duplication mechanisms of VuJMJ genes. Table S11. Ka, Ks values, Ka/Ks ratio, and number of introns for VuSDG and VuJMJ genes duplicated via WGD/Segmental mechanism. Table S12. Species with genomes deposited in the Phytozome database, including their respective families and the number of loci orthologous to VuSDGs. Table S13. Species with genomes deposited in the Phytozome database, including their respective families and the number of loci orthologous to VuJMJs. Table S14. Cis-Regulatory Elements anchored in the promoter regions of VuSDGs and VuJMJs genes, presenting their consensus motifs and associated transcription factors (Matrix JASPAR ID). Table S15. Transcriptional regulation of the VuSDGs identified in the present study. NEX, not expressed; const., constitutive expression; UR, upregulated; DR, downregulated. Table S16. Transcriptional regulation of the VuJMJs identified in the present study. NEX, not expressed; const., constitutive expression; UR, upregulated; DR, downregulated. Table S17. VuSDGs and VuJMJs used in the relative expression analysis, including primer pair sequences, amplicon melting temperatures, and primer pair efficiency values.

Author Contributions: J.B.V.V.: Formal analysis, Investigation, Data Curation, Validation, Writing—Original Draft, Writing—Review and Editing, Visualization; J.R.C.F.-N.: Supervision, Writing—Review and Editing, Methodology, Software; E.B.: Software, Formal analysis; R.L.d.O.S.: Validation, Formal analysis; A.F.d.C.: Methodology; A.M.B.-I.: Supervision, Project administration, Funding acquisition, Writing—Review and Editing. All authors have read and agreed to the published version of the manuscript.

Funding: This research was funded by the Conselho Nacional de Desenvolvimento Científico Tecnológico (CNPq) under grant number 3406048/2022-3, CNPq/MCTI/CT-AGRO No. 32/2022.

Data Availability Statement: The dataset generated for this study can be found online. The repository names and accession numbers are as follows: "https://www.ncbi.nlm.nih.gov/ (accessed on 18 October 2024)", Root dehydration | BioProject ID: PRJNA605156; Mechanical injury + CABMV | BioProject ID: PRJNA655993; Mechanical injury + MV | BioProject ID: PRJNA656211.

Acknowledgments: The authors would like to thank the Fundação de Amparo à Ciência e Tecnologia de Pernambuco (FACEPE), the Conselho Nacional de Desenvolvimento Científico e Tecnológico (CNPq), and the Coordenação de Aperfeiçoamento de Pessoal de Nível Superior (CAPES) for their research scholarships and support. The authors acknowledge the National Laboratory for Scientific Computing (LNCC) for providing high-performance computing resources through the Santos Dumont supercomputer, which were used to obtain part of the results reported.

Conflicts of Interest: Author Eliseu Binneck employed by the Embrapa Soja—Brazilian Agricultural Research Corporation. The remaining authors declare that the research was conducted in the absence of any commercial or financial relationships that could be construed as a potential conflict of interest.

References

1. Kornberg, R.D. Structure of Chromatin. *Ann. Rev. Biochem.* **1997**, *46*, 932–954. [CrossRef] [PubMed]
2. Ferreira-Neto, J.R.C.; Silva, M.; Pandolfi, V.; Crovella, S.; Benko-Iseppon, A.; Kido, E. Epigenetic Signals on Plant Adaptation: A Biotic Stress Perspective. *Curr. Protein Pept. Sci.* **2017**, *18*, 352–367. [CrossRef] [PubMed]
3. Goldberg, A.D.; Allis, C.D.; Bernstein, E. Epigenetics: A landscape takes shape. *Cell* **2007**, *128*, 635–638. [CrossRef] [PubMed]
4. Pfluger, J.; Wagner, D. Histone modifications and dynamic regulation of genome accessibility in plants. *Curr. Opin. Plant Biol.* **2007**, *10*, 645–652. [CrossRef]
5. Ng, D.W.K.; Wang, T.; Chandrasekharan, M.B.; Aramayo, R.; Kertbundit, S.; Hall, T.C. Plant SET domain-containing proteins: Structure, function and regulation. *Biochim. Biophys. Acta* **2007**, *1769*, 316–329. [CrossRef] [PubMed]
6. Bannister, A.J.; Kouzarides, T. Regulation of chromatin by histone modifications. *Cell Res.* **2011**, *21*, 381–395. [CrossRef]
7. Kouzarides, T. Chromatin modifications and their function. *Cell* **2007**, *128*, 693–705. [CrossRef]
8. Chen, X.; Hu, Y.; Zhou, D.X. Epigenetic gene regulation by plant Jumonji group of histone demethylase. *Biochim. Biophys. Acta* **2011**, *1809*, 421–426. [CrossRef]
9. Elkins, J.M.; Hewitson, K.S.; McNeill, L.A.; Seibel, F.; Schlemminger, I.; Pugh, C.W.; Ratcliffe, P.J.; Schofield, C.J. Structure of factor-inhibiting hypoxia-inducible factor (HIF) reveals mechanism of oxidative modification of HIF-1 alpha. *J. Biol. Chem.* **2003**, *278*, 1802–1806. [CrossRef]
10. Trewick, S.C.; McLaughlin, J.; Allshire, R.C. Methylation: Lost in hydroxylation? *EMBO Rep.* **2005**, *6*, 315–320. [CrossRef]
11. Klose, R.J.; Kallin, E.M.; Zhang, Y. JmjC-domain-containing proteins and histone demethylation. *Nat. Rev. Genet.* **2006**, *7*, 715–727. [CrossRef] [PubMed]
12. Jones, M.A.; Morohashi, K.; Grotewold, E.; Harmer, S.L. Arabidopsis JMJD5/JMJ30 acts Independently of LUX ARRHYTHMO within the plant circadian clock to enable temperature compensation. *Front. Plant Sci.* **2019**, *10*, 57. [CrossRef] [PubMed]
13. Huang, S.; Zhang, A.; Jin, J.B.; Zhao, B.; Wang, T.-J.; Wu, Y.; Wang, S.; Liu, Y.; Wang, J.; Guo, P.; et al. Arabidopsis histone H3K4 demethylase JMJ17 functions in dehydration stress response. *New Phytol.* **2019**, *223*, 1372–1387. [CrossRef]
14. Liu, G.; Khan, N.; Ma, X.; Hou, X. Identification, evolution, and expression profiling of histone lysine methylation moderators in *Brassica rapa*. *Plants* **2019**, *8*, 526. [CrossRef]
15. Qian, Y.; Chen, C.; Jiang, L.; Zhang, J.; Ren, Q. Genome-wide identification, classification and expression analysis of the JmjC domain-containing histone demethylase gene family in maize. *BMC Genom.* **2019**, *20*, 256. [CrossRef]
16. Sun, Z.; Wang, X.; Qiao, K.; Fan, S.; Ma, Q. Genome-wide analysis of JMJ-C histone demethylase family involved in salt-tolerance in *Gossypium hirsutum* L. *Plant Physiol. Biochem.* **2021**, *158*, 420–433. [CrossRef]
17. Yan, L.; Fan, G.; Li, X. Genome-wide analysis of three histone marks and gene expression in *Paulownia fortunei* with phytoplasma infection. *BMC Genom.* **2019**, *20*, 234. [CrossRef]
18. Huang, Y.; Liu, C.; Shen, W.; Ruan, Y. Phylogenetic analysis and classification of the Brassica rapa SET domain protein family. *BMC Plant Biol.* **2011**, *11*, 175. [CrossRef]
19. Lu, Z.; Huang, X.; Ouyang, Y.; Yao, J. Genome-wide identification, phylogenetic and co-expression analysis of OsSET gene family in rice. *PLoS ONE* **2013**, *8*, e65426. [CrossRef]
20. Aiese, C.R.; Sanseverino, W.; Cremona, G.; Ercolano, M.R.; Conicella, C.; Consiglio, F.M. Genome-wide analysis of histone modifiers in tomato: Gaining an insight into their developmental roles. *BMC Genom.* **2013**, *14*, 57.
21. Qian, Y.; Xi, Y.; Cheng, B.; Zhu, S.; Kan, X. Identification and characterization of the SET domain gene family in maize. *Mol. Biol. Rep.* **2014**, *41*, 1341–1354. [CrossRef] [PubMed]
22. Xu, J.; Xu, H.; Liu, Y.; Wang, X.; Xu, Q.; Deng, X. Genome-wide identification of sweet orange (*Citrus sinensis*) histone modification gene families and their expression analysis during the fruit development and fruit-blue mold infection process. *Front. Plant Sci.* **2015**, *6*, 607. [CrossRef] [PubMed]
23. Han, Y.; Li, X.; Cheng, L.; Liu, Y.; Wang, H.; Ke, D.; Yuan, H.; Zhang, L.; Wang, L. Genome-wide analysis of soybean jmjc domain-containing proteins suggests evolutionary conservation following whole-genome duplication. *Front. Plant Sci.* **2016**, *7*, 1800. [CrossRef]
24. Fan, S.; Wang, J.; Lei, C.; Gao, C.; Yang, Y.; Li, Y.; An, N.; Zhang, D.; Han, M. Identification and characterization of histone modification gene family reveal their critical responses to flower induction in apple. *BMC Plant Biol.* **2018**, *18*, 173. [CrossRef]
25. Huang, Y.; Mo, Y.; Chen, P.; Yuan, X.; Meng, F.; Zhu, S.; Liu, Z. Identification of SET domain-containing proteins in *Gossypium raimondii* and their response to high temperature stress. *Sci. Rep.* **2016**, *6*, 32729. [CrossRef]

26. Zhang, J.; Feng, J.; Liu, W.; Ren, Z.; Zhao, J.; Pei, X.; Liu, Y.; Yang, D.; Ma, X. Characterization and stress response of the jmjc domain-containing histone demethylase gene family in the allotetraploid cotton species *Gossypium hirsutum*. *Plants* **2020**, *9*, 1617. [CrossRef]
27. Batra, R.; Gautam, T.; Pal, S.; Chaturvedi, D.; Rakhi; Jan, I.; Balyan, H.S.; Gupta, P.K. Identification and characterization of SET domain family genes in bread wheat (*Triticum aestivum* L.). *Sci. Rep.* **2020**, *10*, 14624. [CrossRef]
28. Freire- Filho, F.R. *Feijão-Caupi no Brasil: Produção, Melhoramento Genético, Avanços e Desafios*, 1st ed.; Embrapa Meio-Norte: Teresina, Brazil, 2011.
29. Boukar, O.; Fatokun, C.A.; Huynh, B.L.; Roberts, A.; Close, T.J. Genomic tools in cowpea breeding programs: Status and perspectives. *Front. Plant Sci.* **2016**, *7*, 757. [CrossRef]
30. Lonardi, S.; Muñoz-Amatriaín, M.; Liang, Q.; Shu, S.; Wanamaker, S.I.; Lo, S.; Tanskanen, J.; Schulman, A.H.; Zhu, T.; Luo, M.-C.; et al. The genome of cowpea (*Vigna unguiculata* [L.] Walp.). *Plant J.* **2019**, *98*, 767–782. [CrossRef]
31. Lu, F.; Li, G.; Cui, X.; Liu, C.; Wang, X.-J.; Cao, X. Comparative Analysis of JmjC Domain-containing Proteins Reveals the Potential Histone Demethylases in Arabidopsis and Rice. *J. Integr. Plant Biol.* **2008**, *50*, 886–896. [CrossRef]
32. Schmutz, J.; McClean, P.E.; Mamidi, S.; Wu, G.A.; Cannon, S.B.; Grimwood, J.; Jenkins, J.; Shu, S.; Song, Q.; Chavarro, C.; et al. A reference genome for common bean and genome-wide analysis of dual domestications. *Nat. Genet.* **2014**, *46*, 707–713. [CrossRef] [PubMed]
33. Zimin, A.V.; Puiu, D.; Hall, R.; Kingan, S.; Clavijo, B.J.; Salzberg, S.L. The first near-complete assembly of the hexaploid bread wheat genome, *Triticum aestivum*. *Gigascience* **2017**, *6*, gix097. [CrossRef] [PubMed]
34. Chen, D.H.; Qiu, H.L.; Huang, Y.; Zhang, L.; Si, J.P. Genome-wide identification and expression profiling of SET DOMAIN GROUP family in *Dendrobium catenatum*. *BMC Plant Biol.* **2020**, *20*, 40. [CrossRef]
35. Liu, C.; Lu, F.; Cui, X.; Cao, X. Histone methylation in higher plants. *Annu. Rev. Plant Biol.* **2010**, *61*, 395–420. [CrossRef]
36. Gu, T.; Han, Y.; Huang, R.; McAvoy, R.J.; Li, Y. Identification and characterization of histone lysine methylation modifiers in *Fragaria vesca*. *Sci. Rep.* **2016**, *6*, 23581. [CrossRef] [PubMed]
37. Cerbin, S.; Jiang, N. Duplication of host genes by transposable elements. *Curr. Opin. Genet. Dev.* **2018**, *49*, 63–69. [CrossRef]
38. Kang, Y.J.; Satyawan, D.; Shim, S.; Lee, T.; Lee, J.; Hwang, W.J.; Kim, S.K.; Lestari, P.; Laosatit, K.; Kim, K.H.; et al. Draft genome sequence of adzuki bean, *Vigna angularis*. *Sci. Rep.* **2015**, *5*, 8069. [CrossRef]
39. Kang, W.H.; Kim, S.; Lee, H.A.; Choi, D.; Yeom, S.I. Genome-wide analysis of Dof transcription factors reveals functional characteristics during development and response to biotic stresses in pepper. *Sci. Rep.* **2016**, *6*, 33332. [CrossRef]
40. Wen, C.L.; Cheng, Q.; Zhao, L.; Mao, A.; Yang, J.; Yu, S.; Weng, Y.; Xu, Y. Identification and characterisation of Dof transcription factors in the cucumber genome. *Sci. Rep.* **2016**, *6*, 23072. [CrossRef]
41. He, Q.; Cai, H.; Bai, M.; Zhang, M.; Chen, F.; Huang, Y.; Priyadarshani, S.V.G.N.; Chai, M.; Liu, L.; Liu, Y.; et al. A soybean bZIP transcription factor GmbZIP19 confers multiple biotic and abiotic stress responses in plant. *Int. J. Mol. Sci.* **2020**, *21*, 4701. [CrossRef]
42. Yang, S.; Xu, K.; Chen, S.; Li, T.; Xia, H.; Chen, L.; Liu, H.; Luo, L. A stress-responsive bZIP transcription factor OsbZIP62 improves drought and oxidative tolerance in rice. *BMC Plant Biol.* **2019**, *19*, 260. [CrossRef] [PubMed]
43. Ramirez-Prado, J.S.; Latrasse, D.; Rodriguez-Granados, N.Y.; Huang, Y.; Manza-Mianza, D.; Brik-Chaouche, R.; Jaouannet, M.; Citerne, S.; Bendahmane, A.; Hirt, H.; et al. The Polycomb protein LHP1 regulates *Arabidopsis thaliana* stress responses through the repression of the MYC2-dependent branch of immunity. *Plant J.* **2019**, *100*, 1118–1131. [CrossRef] [PubMed]
44. Lee, S.; Fu, F.; Xu, S.; Lee, S.Y.; Yun, D.J.; Mengiste, T. Global regulation of plant immunity by histone lysine methyl transferases. *Plant Cell.* **2016**, *28*, 1640–1661. [CrossRef] [PubMed]
45. Ayyappan, V.; Kalavacharla, V.; Thimmapuram, J.; Bhide, K.P.; Sripathi, R.; Smolinski, T.G.; Manoharan, M.; Thurston, Y.; Todd, A.; Kingham, B. Genome Wide Profiling of Histone Modifications (H3K9me2 and H4K12ac) and Gene Expression in Rust (*Uromyces appendiculatus*) infected Common Bean (*Phaseolus vulgaris* L.). *PLoS ONE* **2015**, *10*, e0132176. [CrossRef]
46. Crespo-Salvador, Ó.; Sánchez-Giménez, L.; López-Galiano, M.J.; Fernández-Crespo, E.; Schalschi, L.; García-Robles, I.; Rausell, C.; Real, M.D.; González-Bosch, C. The histone marks signature in exonic and intronic regions is relevant in early response of tomato genes to *Botrytis cinerea* and in miRNA regulation. *Plants* **2020**, *9*, 300. [CrossRef]
47. Gan, E.S.; Xu, Y.; Ito, T. Dynamics of H3K27me3 methylation and demethylation in plant development. *Plant Signal. Behav.* **2015**, *10*, e1027851. [CrossRef]
48. Wang, Q.; Liu, P.; Jing, H.; Zhou, X.F.; Zhao, B.; Li, Y.; Jin, J.B. JMJ27-mediated histone H3K9 demethylation positively regulates drought-stress responses in Arabidopsis. *New Phytol.* **2021**, *232*, 221–236. [CrossRef]
49. Larkin, M.A.; Blackshields, G.; Brown, N.P.; Chenna, R.; McGettigan, A.; McWilliam, H.; Valentin, F.; Wallace, I.M.; Wilm, A.; Lopez, R.; et al. Clustal W and Clustal X version 2.0. *Bioinformatics* **2007**, *21*, 2947–2948. [CrossRef]
50. Saitou, N.; Nei, M. The neighbor-joining method: A new method for reconstructing phylogenetic trees. *Mol. Biol. Evol.* **1987**, *4*, 406–425.

51. Kumar, S.; Stecher, G.; Tamura, K. MEGA7: Molecular Evolutionary Genetics Analysis Version 7.0 for Bigger Datasets. *Mol. Biol. Evol.* **2016**, *7*, 1870–1874. [CrossRef]
52. Hu, B.; Jin, J.; Guo, A.-Y.; Zhang, H.; Luo, J.; Gao, G. GSDS 2.0: An upgraded gene feature visualization server. *Bioinformatics* **2015**, *31*, 1296–1297.
53. Hiller, K.; Schobert, M.; Hundertmark, C.; Jahn, D.; Münch, R. JVirGel: Calculation of virtual two-dimensional protein gels. *Nucleic Acids Res.* **2003**, *31*, 3862–3865. [CrossRef] [PubMed]
54. Yu, C.S.; Chen, Y.C.; Lu, C.H.; Hwang, J.K. Prediction of protein subcellular localization. *Proteins Struct. Funct. Bioinform.* **2006**, *64*, 643–651. [CrossRef] [PubMed]
55. Wang, Y.; Tang, H.; DeBarry, J.D.; Tan, X.; Li, J.; Wang, X.; Lee, T.H.; Jin, H.; Marler, B.; Guo, H.; et al. MCScanX: A toolkit for detection and evolutionary analysis of gene synteny and collinearity. *Nucleic Acids Res.* **2012**, *40*, e49. [CrossRef]
56. Sonnhammer, E.L.; Östlund, G. InParanoid 8: Orthology analysis between 273 proteomes, mostly eukaryotic. *Nucleic Acids Res.* **2015**, *43*, 234–239. [CrossRef]
57. Bailey, T.L.; Elkan, C. Fitting a mixture model by expectation maximization to discover motifs in biopolymers; ISMB-94 Proceedings. *Proc. Int. Conf. Intell. Syst. Mol. Biol.* **1994**, *2*, 28–36.
58. Gupta, S.; Stamatoyannopolous, J.A.; Bailey, T.; Noble, W.S. Quantifying similarity between motifs. *Genome Biol.* **2007**, *8*, R24. [CrossRef]
59. Bastos, E.A.; Nascimento, S.P.D.; Silva, E.M.D.; Freire-Filho, F.R.; Gomide, R.L. Identification of cowpea genotypes for drought tolerance. *Rev. Ciênc. Agronôm.* **2011**, *42*, 100–107. [CrossRef]
60. Rodrigues, E.V.; Damasceno-Silva, K.J.; Rocha, M.M.; Bastos, E.A.; Teodoro, E. Selection of cowpea populations tolerant to water deficit by selection index. *Rev. Ciênc. Agron.* **2017**, *48*, 889–896. [CrossRef]
61. Rodrigues, F.A.; Marcolino-Gomes, J.; Carvalho, J.F.; Nascimento, L.C.; Neumaier, N.; Farias, J.R.; Carazzolle, M.F.; Marcelino, F.C.; Nepomuceno, A.L. Subtractive libraries for prospecting differentially expressed genes in the soybean under water deficit. *Genet. Mol. Biol.* **2012**, *35*, 304–314. [CrossRef]
62. Hoagland, D.R.; Arnon, D.I. The Water-Culture Method for Growing Plants Without soil. Circular. California Agricultural Experiment Station 347. 1950. Available online: https://www.cabdirect.org/cabdirect/abstract/19500302257 (accessed on 20 February 2021).
63. Rocha, M.M.; Lima, J.A.A.; Freire-Filho, F.R.R.; Lima, C.V. Resistencia de Caupi de Tegumento Branco a Algumas Estirpes de Comovirus, Potyvirus e Cucumovirus. 1996. Available online: https://www.alice.cnptia.embrapa.br/handle/doc/53796 (accessed on 20 February 2021).
64. Oliveira, C.R.R.; Filho, F.R.F.; Nogueira, M.S.; Barros, G.B.; Eiras, M.; Ribeiro, V.Q.; Lopes, Â.A. Reação de Genótipos de Feijão-caupi Revela Resistência às Coinfecções Pelo Cucumber Mosaic Virus, Cowpea Aphid-Borne Mosaic Virus e Cowpea Severe Mosaic Virus. 2012. Available online: https://www.alice.cnptia.embrapa.br/handle/doc/940785 (accessed on 20 February 2021).
65. Cardoso, M.J.; Freire-Filho, F.R.; Athayde-Sobrinho, C. *BR 14-mulato: Nova Cultivar de Feijão Macassar Para o Estado do Piauí*; Comunicado Técnico, 48; Embrapa-UEPAE de Teresina: Teresina, Brazil, 1990; p. 4.
66. Barna, B.; Király, L. Host–pathogen relations: Diseases caused by viruses, subviral organisms, and phytoplasmas. *Plant Toxicol.* **2004**, *1*, 533–568.
67. Ferreira-Neto, J.R.C.; da Costa Borges, A.N.; da Silva, M.D.; de Lima Morais, D.A.; Bezerra-Neto, J.P.; Bourque, G.; Kido, E.A.; Benko-Iseppon, A.M. The Cowpea Kinome: Genomic and Transcriptomic Analysis Under Biotic and Abiotic Stresses. *Front. Plant Sci.* **2021**, *12*, 1–22. [CrossRef] [PubMed]
68. Amorim, L.L.B.; Ferreira-Neto, J.R.C.; Bezerra-Neto, J.P.; Pandolfi, V.; de Araújo, F.T.; da Silva Matos, M.K.; Santos, M.G.; Kido, E.A.; Benko-Iseppon, A.M. Cowpea and abiotic stresses: Identification of reference genes for transcriptional profiling by qPCR. *Plant Methods* **2018**, *14*, 88. [CrossRef]
69. Pfaffl, M.W.; Horgan, G.W.; Dempfle, L. Relative expression software tool (REST) for group-wise comparison and statistical analysis of relative expression results in real-time PCR. *Nucleic Acids Res.* **2002**, *30*, e36. [CrossRef]

Disclaimer/Publisher's Note: The statements, opinions and data contained in all publications are solely those of the individual author(s) and contributor(s) and not of MDPI and/or the editor(s). MDPI and/or the editor(s) disclaim responsibility for any injury to people or property resulting from any ideas, methods, instructions or products referred to in the content.